Received: 13 November 2021 | Revised: 5 August 2022 | Accepted: 17 August 2022
DOI: 10.1002/gj.4581

RESEARCH ARTICLE

WILEY

Black shales and mesozonal quartz vein-hosted Au: The Truchas Syncline, Spain and the Harlech Dome, Wales, a comparative study

John Keiller Cunningham[1] | **Fernando Gómez-Fernández**[2] | **Luis González-Menéndez**[3] | **Andrew David Beard**[1]

[1]Department of Earth and Planetary Sciences, Birkbeck College, University of London, London, UK
[2]Área de Prospección e Investigación Minera, Universidad de León, León, Spain
[3]Instituto Geológico y Minero de España, León, Spain

Correspondence
John Keiller Cunningham, Department of Earth and Planetary Sciences, Birkbeck College, University of London, 9 Malet Street, London WC1E 7HX, UK.
Email: j.cunningham@bbk.ac.uk

Funding information
Project 0284_ESMIMET_3_E, belonging to the INTERREG V-A Spain-Portugal Cooperation Programme (2014-2020)

Handling Editor: L. Tang

A comparative study of quartz vein-hosted gold occurrences associated with Palaeozoic metapelites in two areas of Wales and Spain combines new, previously unpublished and published data. Metamorphic grade is greenschist in both areas, but very low-grade indicators in the host metapelites distance the environment from the greenschist/amphibolite transition zone required for some orogenic gold occurrences. Basin fertility for Au is indicated by the presence of auriferous pyrites in the protolith black shales in Spain. Only minor igneous activity has taken place in both study areas. Mineral parageneses are similar, with early sulphide phases characterized by As/Co and later auriferous phases by Cu/Pb/Zn sulphides. Mesozonal P–T conditions apply at deposition in both terranes. In Spain, mineralisation typically occurs in quartzites near to the metapelites, but not where the veins are in contact with them, and extensional faulting appears to be a stronger control over mineralisation than geochemical interaction with metapelite wall-rocks. In Wales, both structural and geochemical factors (C content of the wall-rocks and coupled oxidation of NH_4 ions substituted in wall-rock phyllosilicates to produce CH_4 and N_2) could have a role in Au deposition. In both areas, minor cross-fault systems between larger faults are typical hosts of the mineralisation. Assignment is made to different subtypes of the orogenic gold model but these subtypes share the characteristic of a local source. This has implications for exploration methodology in epizonal/anchizonal metapelite-dominated terranes, where indicators of basin fertility for Au within the protolith itself assume importance.

KEYWORDS
black shales, gold, Harlech, orogenic, Truchas, veins

1 | INTRODUCTION

Orogenic gold deposits (OGDs hereafter), where the gold is sourced from the metamorphic rocks themselves rather than from external sources such as felsic-granitoid intrusives, account for significant gold production, thus >75% of historic production (Tomkins, 2013). Determination of P–T–x conditions applying at deposition enabled an important classification of OGDs into epizonal/mesozonal/hypozonal types (Groves et al., 1998). Within the Phanerozoic OGDs, Mortensen et al. (2022) established four subtypes based on factors which include those with economic significance. Accordingly, the assignment of an OGD to one of these subtypes can be related to its economic potential and determine the appropriate exploration methodology. This paper reports the results of a comparative study of OGDs in two regions, the Truchas Syncline in Spain (Truchas hereafter) and the Harlech Dome in Wales (Harlech hereafter) (Figure 1). Both are Phanerozoic OGD districts within which quartz vein-hosted Au occurs in or near to meta-sedimentary sequences containing black shales

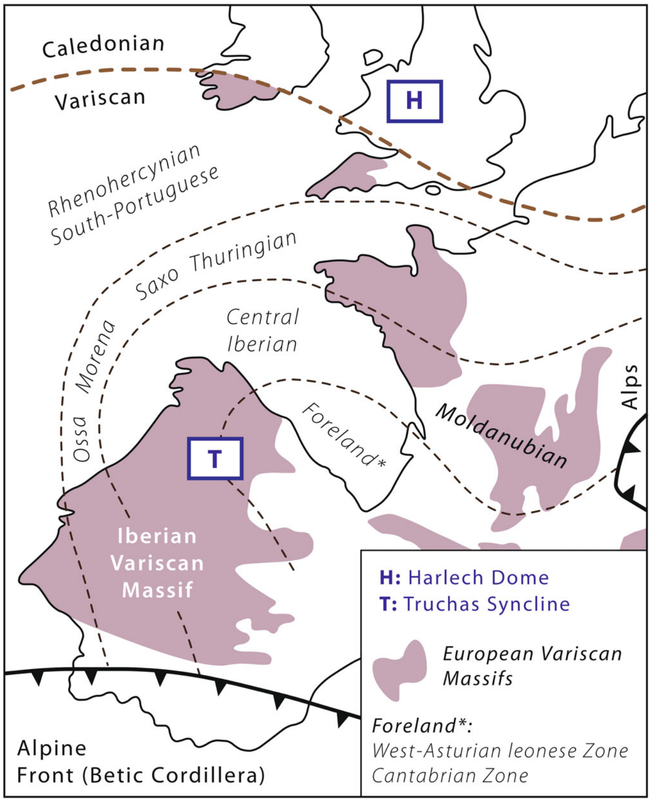

FIGURE 1 Regional setting and location of the study areas

(Huyck, 1990), an OGD association with a relatively long history of investigation (Gaboury, 2021; Keppie et al., 1986). Both study areas occur where, pre-basin inversion, Palaeozoic depositional basins have hosted anoxic/euxinic conditions from time to time, where post-basin inversion, sedimentary and tectonic burial has led to the formation of slates, and where the mobilization of hydrothermal fluids under meso-zonal conditions has led to gold mineralisation within an orogenic environment. Metamorphic grade is at greenschist facies, with some very low grades (anchizonal) in Harlech. There are no major granitoid intrusions exposed at surface; only minor exposures of igneous rocks of a range of compositions occur within the sedimentary sequence in both areas.

If there are no potential magmatic sources (as in our study areas), it is the levels of gold in basin sediments pre-inversion which constrains the economic potential of the post-inversion processes (transportation, concentration and deposition). The concept of basin fertility (Pitcairn et al., 2017, 2021; Sack et al., 2018) becomes important. Studies of processes prior to inversion of the basin sediments during diagenesis and very low-grade metamorphism have provided valuable insights into basin fertility for Au. Thus, a role for diagenetic framboidal pyrite in "carbonaceous" sediments is proposed for the capture and subsequent concentration of Au during subsequent changes from framboidal to euhedral pyrite (Large et al., 2011, Section 5).

Gold captured in basin sediments is subject to subsequent processes which are critical in the transportation, concentration and deposition of economic Au deposits. The model proposed for the Welsh gold belt (the Harlech model hereafter) involves C and NH_4, released by intense alteration of wall-rock black shales, interacting with an externally derived auriferous hydrothermal fluid, which results in gold deposition (Bottrell & Miller, 1990; Naden & Shepherd, 1989; Shepherd & Bottrell, 1993). In similar black shale environments, the concentration of gold to economic levels may be subordinate to other factors, such as the size of the hydrothermal cell, repeated fluctuations in fluid pressure, and shear stress associated with fault-valve behaviour (Bierlein et al., 2001; Cox et al., 1995; Jahoda et al., 1989; Sibson et al., 1988). Post basin inversion, a model for scavenging of gold during pervasive metamorphic devolatilization of whole sedimentary sequences (Pitcairn et al., 2006; Pitcairn et al., 2015) and for pelites specifically (Zhong et al., 2015) during prograde metamorphism to at least amphibolite facies, generates Au-bearing fluids with minor enrichment in Pb, Zn and Cu. This successfully replicates the "gold-only" nature of economic deposits of orogenic gold (Pokrovski et al., 2014). It does not however explain the presence and significance of CO_2 levels in fluids/volatiles associated with gold deposits (Hu et al., 2017; Phillips & Evans, 2004), including those classified as OGDs. The greenschist/amphibolite transition implies temperatures generally >550°C (Finch & Tomkins, 2017; Pitcairn et al., 2006; Pitcairn et al., 2015). Much lower temperatures are reported from OGDs hosted by sub/lower/upper greenschist-grade meta-sedimentary sequences similar to our study areas containing black shales (Kříbek et al., 2015; Wu et al., 2019).

The structure of the paper follows the comparative study methodology (Carpi & Egger, 2008). Thus (a) we compare the ore settings in Harlech and Truchas to identify key differences, (b) we test the models (the Harlech model and the Large et al., 2011 model) which the key differences identified under (a) suggested were the most relevant to the mineralisation processes in orogenic settings for OGDs, specifically where black shales (metapelites) occur in proximity to mineralised quartz veins, and (c) we classify the deposits according to the OGD subtypes proposed by Mortensen et al. (2022), with implications for their economic potential.

The paper also provides context to more detailed work we have published elsewhere on the role of CO_2 (González-Menéndez et al., 2021) and on the gold-bearing framboidal pyrite we report from Truchas (Gómez-Fernández et al., 2019, 2021).

2 | GEOLOGICAL SETTING

The geological settings within which the Au mineralisation occurs in both Harlech and Truchas are broadly similar (Figures 2, 4). A summary of comparative geological features is given in Table 1.

2.1 | Harlech

As summarized in Table 1, the Harlech Dome was formed as Palaeozoic siliclastic basin sediments suffered inversion during the

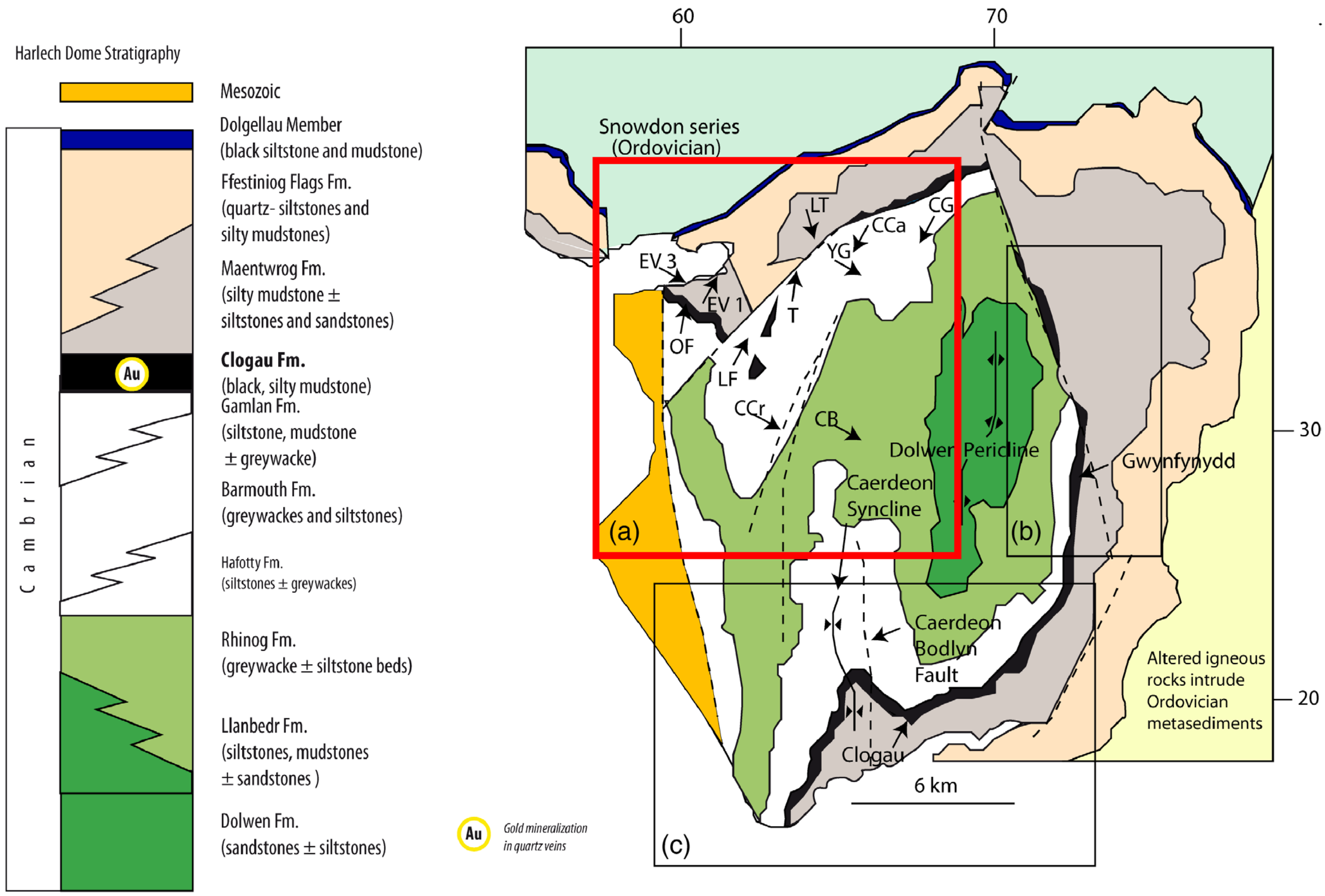

FIGURE 2 The Cambrian succession on the Harlech Dome with the "meridional faults" and the location of the northern gold belt (b) and southern gold belt (c). The red box outlines the area of the Harlech Dome where new samples were collected (e.g., OF) for this paper. (based on BGS map data, with permissions CP22/019 BGS copyright UKRI 2022. The BGS 1:50000 sheets are named in references (British Geological Survey, 1997, Institute of Geological Sciences, 1978)). Data S5 (Appendix 1) provides precise locations

Caledonian Orogeny in the Silurian, when movement on long-lived "meridional" faults (Shepherd & Bottrell, 1993) combined with large-scale open folding to create an anticlinal form, the Dolwen pericline, as modified by the Caerdeon Syncline (Figure 2). Faulting has exerted a strong control over geological history; the term Harlech Horst is used (e.g., Mason et al., 1999) to reflect the early phase of faulting which created the generally N-trending "meridional" faults. A black metapelite, the Clogau Fm, outcrops around the structure and later in basin history, black metapelite occurs again as the Dolgellau Fm. The Welsh gold belt (Hall, 1990; Morrison, 1975), where gold has been mined since the 19th Century, follows the southern and eastern outcrop of the Clogau Fm (Figure 2b,c). Total production of the Welsh gold belt is small, estimated at a little in excess of 150,000 ounces (Platten & Dominy, 2009) with highly localized "bunches" of visible gold in quartz.

In Harlech, an auriferous "quartz vein" in the gold belt is typically a number of individual quartz veins, interleaved with country rock sheets, with a total thickness up to 6 m (Platten & Dominy, 1999), and attributed to dilatant fracturing (Gilbey, 1968; Mason et al., 2002). This pattern is repeated in our new study area but total thickness extends only up to 0.5 m (Ogof Foel, Figure 2, 3a, Data S4A). In the gold belt, a major problem for the miners was that the veins are non-auriferous over considerable strike lengths, with only very localized and very rich "bunches" (Hall, 1990), assaying up to 5667 ppm Au (Platten & Dominy, 2009). The recognition that the mineralisation may predate the metamorphic hiatus/cleavage development (Mason et al., 1999; Platten & Dominy, 1999) further distinguishes these potentially auriferous quartz veins, from the barren "metamorphic" quartz veins which also occur and late stage barren carbonate veins (Figure 10, Ceunant Geifr in Data S4A).

2.2 | Truchas

The Truchas Syncline (Figure 4) is located on the NW margin of the Central Iberian Zone. Here the limits of this tectonostratigraphic zone with the northern domains are marked by Variscan thrust structures. As summarized in Table 1, Truchas has similar geological features to Harlech, with the Luarca Fm, a black metapelite, (Suárez et al., 1994) outcropping round the structure. Metapelites are the dominant rock type throughout the M-U Ordovician and Silurian succession in the Truchas (Figure 4). However, there is greater structural complexity in

TABLE 1 Comparative geological features between the Harlech Dome and the Truchas Syncline

Geological features	Sediment age	Deformation age	Main structure	Met. Min	Met. Grade	C.M.	Vein-type	Volcanics and setting
HARLECH (Clogau FM.)	Cambrian	Caledonian 490–390 Ma	Anticline dome	Chlorite Muscovite ±Quartz ±Albite	Greenschists	C ≈ 0.69%	Quartz	Andesites greenstones Arc-derived
TRUCHAS Spain (Luarca FM.)	Ordovician to Silurian	Variscan 350–300 Ma	Syncline	Chlorite Muscovite ±Quartz ±Albite	Greenschists	C ≈ 0.24%	Quartz ±Calcite	Basalts ±Dacites/ ±Rhyolites Rift-derived

Abbreviations: C.M., carbonaceous material in black shales; Met.Min, metamorphic minerals.

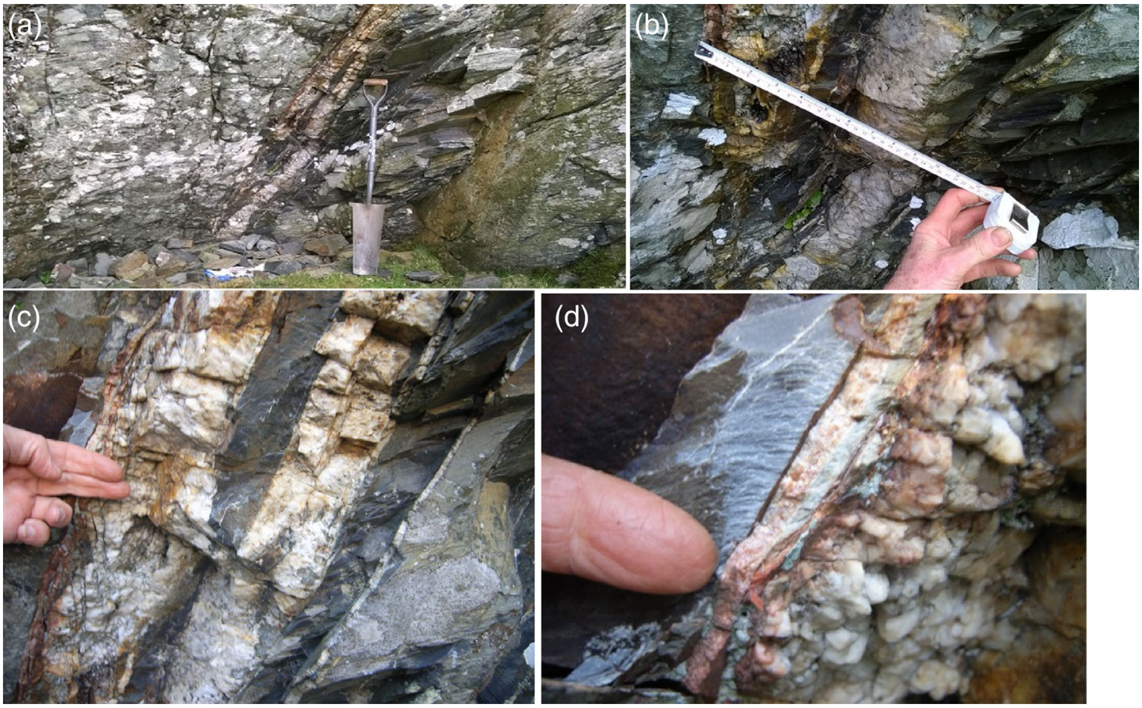

FIGURE 3 Ogof Foel vein. Images in (a) to (c) demonstrate discontinuous major/minor quartz lenses with Clogau shale interleaves. The margin in (d) is sharp and shows no sign of alteration

the Spanish study area (Fernández, 2001) and as reported from further west (Fernández et al., 2007). Isoclinal D1 folding, D2 thrust structures and D3 open folding impose a regional trend of 110° E, the axis of the Truchas Syncline.

Later deformation forming the present structure is asymmetric, with the northern flank becoming more vertical towards the northern boundary where erosion exposes a prominent quartzite formation (Armorican Quartzite) (Figure 4). Locally, the contact between shales (Luarca Fm) and quartzites (Armorican Quartzite) is often inverted by multiple minor folds.

The fault pattern (Figure 4) in the west of the Truchas Syncline is on the regional trend, cut by cross-faults at ≈90°. In the central/eastern and southern area, an ENE trending set are dominant, with a cross-fault suite, again at ≈90°, some identified as thrusts (Fernández-Lozano et al., 2016).

On a much more local scale, groups of N-S quartz veins with an extensional pattern occur (Llamas de Cabrera and Manzaneda), (Figure 5a,d). Multiple thin mineralised crush zones follow the regional 110° E fault trend (Figure 5e,f,g). The country rock is Armorican quartzite, with the exception of Machato (Figure 5a) and Pozos (Figure 4), where the Luarca Fm hosts veins and a stockwork respectively. The quartzite contains scarce minor non-quartz grains showing silicification, chloritization, and sericitization, within 1 m thick alteration zones. In marked contrast to the fault-related auriferous veins described above, at Cunas, quartz veins are disorderly and appear to follow no structural pattern (Figure 6, Data S3).

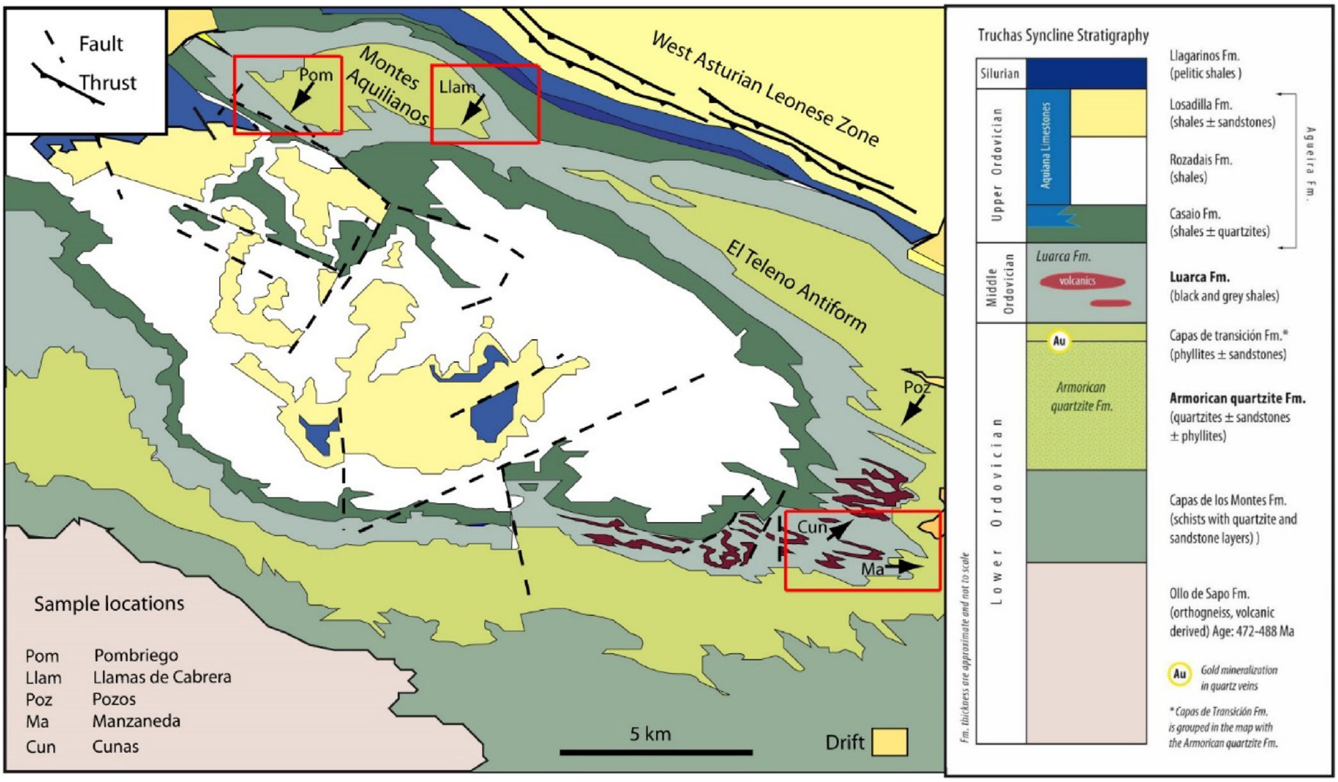

FIGURE 4 The Truchas Syncline, with the metapelite-dominated sequence from the Luarca Formation to the Pizarras de Llagarinos (from InfoIGME website and Voldman & Toyos, 2019, see references). From left to right in red boxes: Pombriego, Llamas de Cabrera and Cunas-Manzaneda are areas investigated in detail in this paper (and detailed in Figure 5). The precise location of new samples from these sites and Pozos are given in Data S5

3 | METHODS

3.1 | Sampling

Quartz veins were sampled in an area of Harlech (Figure 2a), where "mineralised veins" are marked on BGS 1:50000 Sheets named in References (Institute of Geological Sciences, 1978), the association of black shales (Clogau Fm) and greenstones (mafic volcanic rocks) were present and no significant mining had taken place historically. The sampling done was normally restricted to where metal sulphides occur, typically in a quartz vein, less typically a brecciated zone. Since the sample locations (Figure 2a) are outside the main gold belt (Figure 2b,c), where the key mines of Gwynfynydd and Clogau-St Davids are located, they provide an opportunity to test models with new data collected from near a well-documented area (Gilbey, 1968; Hall, 1990; Mason et al., 1999, 2002; Morrison, 1975; Platten & Dominy, 1999, 2009; Shepherd & Bottrell, 1993), A similar opportunity is presented in Truchas, where discovery of in-place Au (Gómez-Fernández et al., 2005; Gómez-Fernández, Vindel, González Clavijo, et al., 2012; Gómez-Fernández, Vindel, Martín-Crespo, et al., 2012) occurs in an area where large-scale alluvial gold mining by the Romans is documented (Fernández-Lozano et al., 2015; Gómez-Fernández et al., 2005; Herail, 1984). The field work was conducted in three areas (Pombriego, Llamas de Cabrera and Cunas-Manzaneda), (Figure 4). The area of Manzaneda was sampled where primary gold-bearing quartz had been reported (Fernández-Lozano et al., 2015). A search was made for mineralised quartz veins at Cunas (Figure 4), where outcrops of shales contain mafic ± felsic igneous rocks (Suárez et al., 1994), similar to mafic volcanics studied further to the north (Villa et al., 2004). In the Pombriego area (Figure 5e), sampling required detailed geological mapping to resolve issues relating the mineralisation to the local geological structure.

3.2 | Laboratory

Quartz samples were split and one half were analysed for Au by ALS Laboratories in Galway using fire assay techniques with AAS (atomic absorption spectrometry) detection, imposing a detection limit of 0.01 ppm. In total, 43 samples were assayed, 21 from Harlech and 22 from Truchas. The other half were prepared for optical, SEM (scanning electron microscopy) and EMPA (electron microprobe analysis) studies at the School of Mines, University of Leon and at Birkbeck College, University of London. At Birkbeck College, major-element mineral analyses were conducted using a Jeol JXA8100 Superprobe with an Oxford Instruments AZtec system (EDS). Analysis was carried out using an accelerating voltage of 15 kV, a current of 1 μA and a

FIGURE 5 Truchas quartz veins. (a) and (b) extensional N-S quartz veins at llamas de Cabrera; (c) and (d) extensional N-S quartz veins at Manzaneda, where 7 quartz veins are seen within 12 m; (e) Pombriego mines on the regional 110° E fault trend (f) Pombriego mine portal with mineralised crush zone; (g) near Pombriego Village level multiple thin mineralised crush zones cutting thick quartzites. (precise locations in Data S5 and further details in Data S3)

beam diameter of 1 μm. The analyses were calibrated against standards of natural silicates, oxides and Specpure metals, with the data corrected using a ZAF programme. At León University a JEOL JSM-6480 scanning electron microscope (SEM), equipped with an Oxford D6679 EDS detector, and an Olympus BX51 petrographic microscope (MOP), equipped with an Olympus Camedia C-5050 Zoom lens double bed, was employed for microscopic characterization.

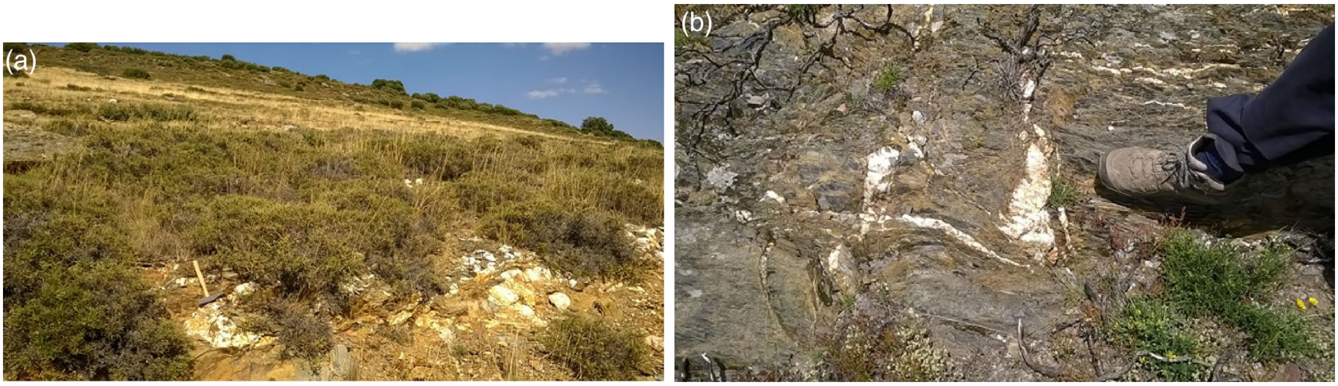

FIGURE 6 Vein quartz at Cunas. (a) Vein up to ≈1 m thick in foreground, quartz is present in the float across the background área; (b) minor veins parallel to and cross-cutting cleavage

4 | THE QUARTZ VEINS

4.1 | Mineral paragenesis, fluid inclusion data and P–T conditions during ore deposition; the mesozonal context

Historic data for key localities in Harlech and Truchas are summarized in Table 2, together with the source references.

Generally, the mineral paragenesis in the quartz veins is typical of the orogenic gold environment. An early phase carrying the indicator mineral arsenopyrite is followed by the productive Au phase where arsenopyrite may be absent and the base metal sulphides (Pb, Zn, Cu) dominate the paragenesis, but at sub-economic levels, hence "gold-only" (Pokrovski et al., 2014). Free gold was located in microfractures in both areas. Within highly localized zones in the Welsh gold belt, levels of visible free gold were dramatically high but exceptional (Hall, 1990; Morrison, 1975). In Harlech, early Fe (pyrite)–Co–As assemblages followed by Au–Ag–Bi–Te–Pb-Sb, then Cu–Fe (pyrrhotite) predominate, with the final stage dominated by Pb–Zn. In Truchas, the paragenesis is similar, but two phases of arsenopyrite were recognized (Gómez-Fernández et al., 2005). Fluid inclusion studies highlight important differences between Harlech and Truchas. Within the productive Au phase, the Harlech fluid inclusions contain "methanoic" CH_4 and N_2 (5% CO_2) species, as well as aqueous inclusions, in contrast to the aqueous only species within the Truchas productive Au phase. The aqueous only species from Truchas reflects the regional pattern of auriferous fluids which are reported from NW Iberia (Boiron et al., 1996; Noronha et al., 2000), which have very low salinities attributed to dilution by meteoric waters (Boiron et al., 2003). In Truchas, fluid inclusion and arsenopyrite geothermometer studies (Gómez-Fernández, Vindel, Martín-Crespo, et al., 2012) identified that P–T conditions were favourable for arsenopyrite and pyrite deposition in quartz veins from aqueous-carbonic fluids at 300–390°C and 2–2.2 kbar. The stage of gold precipitation from aqueous fluids occurred towards 180–310°C and 2.0 kbar. These studies enabled the identification of three hydrothermal stages: As–Fe (I), As–Fe (II), and Au–Zn–Cu–Pb. Fluid inclusions from hydrothermal quartz in the Clogau-St Davids gold mine indicate conditions of formation of 300–320°C and 1.8 kbar (Bottrell et al., 1988). Thus, the context for the Au mineralisation is at the lower end of mesozonal P–T conditions in both study areas areas, sensu Groves et al. (1998).

4.2 | Isotope data

In Truchas, the $\delta^{34}S$ values (Gómez-Fernández, Vindel, Martín-Crespo, et al., 2012) are similar for the two As–Fe stages described above (+8.0‰ to +16.3‰ and +9.0‰ to +19.5‰ respectively) and for pyrites from the Luarca Fm (+7.4‰ to +26.3‰), suggesting a comparable S source. In Harlech (Shepherd & Bottrell, 1993), the $\delta^{34}S$ levels in overlying Maentwrog Fm country rocks are +17.7‰ to +20.4‰ compared to +5.5‰ to +7.7 ‰ in the underlying Clogau Fm which mainly hosts the auriferous quartz veins. The $\delta^{34}S$ levels in vein sulphides crossing these formations were +9.8‰ to +11 ‰ and −2.5‰ to +5.2‰ respectively. The Bryn-Teg borehole which encountered volcanic basement on the Harlech Dome yielded $\delta^{34}S$ values of +3.7‰ (Smith & McCann, 1978). This data, addition of Cr and Ni to altered basic intrusive wall-rocks, together with chlorites which are Mg-rich and Mn-poor, led the authors to argue that an auriferous hydrothermal fluid with $\delta^{34}S$ values of 0‰ was generated from a basic-ultrabasic intrusion in the basement below. There is some geophysical evidence for this intrusion (Smith & McCann, 1978).

4.3 | Assay data and supporting petrographic studies

Gold content of vein quartz, field observations, and supporting petrographic studies from the areas sampled in this study are now summarized in Tables 3 and 4. The results from optical, SEM, EMPA and AAS studies are supportive of the mineral paragenesis summarized in Table 2.

TABLE 2 Early and productive Au phase mineral paragenesis and fluid inclusion types from key localities in the study areas

	Mineral	Gwynfynydd	Clogau – St Davids	Llamas de Cabrera district
Productive Au phase	Quartz	X	X	X
	Calcite	X	X	
	Gold	X	X	X
	Pyrite	X	X	
	Cobaltite	X		
	Pyrrhotite	X	X	X
	Chalcopyrite	X	X	X
	Sphalerite	X	X	X
	Galena	X	X	X
	Bismuthinite	X	X	
	Tellurides	X	X	
	Tetrahedrite			X
	Fluid inclusions			
	Aqueous	X	X	X
	CH_4 and N_2 (5% CO_2)	X	X	
Early phase	Quartz	X	X	X
	Calcite	X		
	Pyrite	X		X
	Arsenopyrite	X		X
	Pyrrhotite		X	
	Cobaltite		X	
	Bismuthinite			X
	Fluid inclusions			
	CO_2-(CH_4)			X
	Aqueous-carbonic[a]			X

Note: Data for Gwynfynydd and the Clogau-St Davids mines from Bottrell et al. (1988), Mason et al. (1999), Mason et al. (2002), Shepherd and Bottrell (1993). Data for Llamas de Cabrera from Gómez-Fernández et al. (2005), Gómez-Fernández, Vindel, Martín-Crespo, et al. (2012).
[a]Liquid and vapour phase CO_2.

4.3.1 | Harlech

The productive Au phase mineral assemblages, and the early phase assemblages, including cobaltite as well as arsenopyrite, were found in our new study area. In the optical microscopy and SEM images (Figures 7a,b, Data S4A and S4B), euhedral arsenopyrite precedes galena and late dolomite. The diagonal country rock shard (Figure 7a) includes dolomite and two generations of chlorite, a bluish and also a yellowish type associated with white mica. The rock (Figure 7d) comprises large quartz crystals with subdomains which show undulating extinction, with small chalcopyrite grains at the margins. Large sphalerite grains contain chalcopyrite, galena and an idiomorphic cobaltite grain (Figure 7c).

The wall-rocks hosting the veins sampled for this project extend from the Rhinog Grits upwards to the Maentwrog Fm (Figure 2). However, unlike in the gold belt, no wall-rock alteration was observed. Gold levels assayed were low. Where presence of the base metal sulphides (Pb, Zn and Cu) and absence of arsenopyrite indicate productive Au phase mineralisation, the assays (Table 3) returned the highest value for the Harlech terrane at 0.22 ppm Au (Estuary vein 3, Data S4A). This vein was hosted in the overlying Maentwrog Fm, rather than the Clogau Fm. Of the remaining 6 localities which provided values at or above 0.02 ppm (the level often taken as anomalous in Au mining exploration), only one was in the favoured shale-dominated Clogau Fm and the remaining 5 veins hosted in the underlying Gamlan Fm (Figure 2). These data contrast with the gold belt; the Gamlan Fm, dominated by greywacke with shales/silts only occurring within interbeds, was only productive at three locations during the height of the gold belt activity (Platten & Dominy, 2009).

4.3.2 | Truchas

The new assay data collected, together with data previously collected (Gómez-Fernández, Vindel, González Clavijo, et al., 2012) from Llamas

TABLE 3 Summary of assay work on samples collected in Harlech

Location[a]	Sample	Wallrock	Host	Field observations	Au (ppm)
Llyn Tecwyn (LT)	L225707	Maent	Qtz	Vuggy Fe stained milky qtz	0.01
	L225708	Maent	Qtz		0.01
	L225709	Maent	Qtz	Qtz, gn, cpy, py,	0.01
Estuary vein 1 (EV1)	E001	Maent	Qtz	Minor py, altered qtz, Fe-stained	0.01
Estuary vein 3 (EV3)	E006	Maent	Qtz	Ox, milky qtz, minor py, 5% cpy	0.22
Ceunant Geifr (CG)	L225710	Gamlan	Dmt	Py, cpy, bo	0.01
Ogof Foel (OF)	L225711	Clogau	Qtz	Vuggy qtz, fe-stained	0.01
	L225712	Clogau	Qtz	Hm, vuggy qtz	0.07
	E002	Clogau	Qtz	Dull grey qtz	0.01
Y Gyrn (YG)	L225713	Gamlan	Shale	Qtz, chl, py, other phyllosilicates	0.01
	L225714	Gamlan	Qtz	Qtz, py, cpy, malachite	0.09
	L225715	Gamlan	Qtz	Py, cpy, glassy qtz	0.02
	L225716	Gamlan	Qtz	Qtz, py, cpy, bo	0.03
Coed Caerwych (CCa)	L225717	Gamlan	Qtz	Glassy qtz, py, gn, cpy, co	0.01
Coed Crafnant (CCr)	L225718	Gamlan	Bx	Ox, bx, hm, py, qtz	0.01
	L225719	Gamlan	Shale	Ox, py	0.01
	L225720	Gamlan	Qtz	Massive cpy in qtz boulder in spoil	0.02
Cwm Bychan (CB)	L225721	Rhinog	Qtzbx	Ox. Qtz, bx, minor py, weathered, vuggy	0.01
	L225722	Rhinog	Qtzbx	Crush zone, ox. Qtz, bx	0.01
Lletty'r-Fwyalch (LF)	L225723	Gamlan	Qtz	Qtz py	0.04
	L225724	Gamlan	Qtz	Qtz py	0.01
Talsarnau (T)	L225725	Gamlan	Qtz	60 cm qtz vein	0.01

Note: Au (ppm) levels determined using fire assay techniques with AAS detection, detection limit 0.01 ppm. Data S4A and S4B provides field and laboratory detail. Precise locations are given in Data S5.
Abbreviations: apy, arsenopyrite; bo, bornite; bx, breccia; chl, chlorite; co, cobaltite; cpy, chalcopyrite; dmt, dolomite; gn, galena; hm, haematite; Maent, Maentwrog; ox, oxidized; py, pyrite; qtz, quartz.
[a]In brackets acronyms as shown in Figure 2 and listed in Appendix 1 (Data S5).

de Cabrera, Pombriego and Pozos are included in Table 4. With three exceptions, samples are from veins in the Armorican Quartzite Fm, near to the contact with the younger black shales, the Luarca Fm. The three exceptions, Machato, Cunas and Pozos, are from quartz veins in the Luarca Fm. Where quartz, as observed in the field, contained no other minerals (sulphides, oxides, lithics), Au levels were at or less than detection level. Where other minerals were observed in the field, in particular arsenopyrite/pyrite, Au contents range up to 18.7 ppm (Table 4).

At Cunas, while pyrite was present in the veins (Figure 8e), neither arsenopyrite nor Au was detected. The idiomorphic pyrite occurs at the margins of the coarse quartz grains which make up the rock (Figure 8b), and creates a texture which contrasts strongly with that of the fine-grained multiple quartz veins in the gold-bearing sample at Manzaneda (Table 4, 45, Figure 8a).

Regarding wall-rock alteration, silicification, chloritization and sericitization in localized areas of the enclosing rocks has been reported from Truchas (Gómez-Fernández, Vindel, Martín-Crespo, et al., 2012) where the typical Au host rock is a relatively pure quartzite with a sparse heavy mineral assemblage.

5 | THE BLACK SHALES AND AU: METAMORPHIC GRADE, TOC CONTENT AND THE FE SULPHIDES WITHIN THEM

For black shale-hosted gold mineralisation, where there is no evidence of intrusion-related processes, the need to take a more complete view of the basin history to account for Au capture, release, transportation and deposition processes has been stated (Large et al., 2011). The sequence of processes proposed can be summarized as.

1. capture of Au, As and other metals by the formation of organometallic complexes with organic matter (OM hereafter) within basin muds below a basal anoxic-euxinic layer within the seawater column.
2. early diagenesis of the muds, when the OM may partially dissolve, releasing the metals to be incorporated in diagenetic pyrite (which often displays framboidal textures)
3. late diagenesis and early metamorphism, when the oil window is passed and OM migrates. A second generation of pyrite may replace the earlier diagenetic pyrite, with resulting release of some Au to pore waters.

TABLE 4 Summary of assay work on samples from Truchas

Sample		Wallrock	Location	Host	Field observations	Au ppm
Data from the present work	43	Arm	Man	Qtz	From fold hinge, no sulphides	<0.01
	44	Arm	Man	Qtz	From cross-fault, no sulphides	<0.01
	45	Arm	Man	Qtz	qtz apy	0.68
	46	Arm	Man	Qtz	qtz from trial	0.01
	E003	Arm	Pom Vill	Qtz	milky qtz, 70% py	3.10
	E004	Arm	Pom Mine	Qtz	milky ox. qtz, 2% gn	0.04
	E005	Luarca	Pozos	Qtz	ox. milky qtz, minor py, 5% cpy	0.33
	E007	Luarca	Cunas	Qtz	Milky qtz, py	0.01
Data from Gómez-Fernández, Vindel, González Clavijo, et al. (2012)	31	Arm	Pom Mine	Qtz	qtz, apy, py	3.52
	PZ	Arm	Pozos	Qtz	qtz, apy	0.50
	M31	Arm	La Casarina	Qtz	qtz, apy	18.70
	132B	Arm	La Casarina	Qtz	qtz, apy	5.19
	M12	Arm	La Casarina	Qtz	clays in contact with a qtz v.	<0.03
	M2	Luarca	Machato	Qtz	qtz, shale	2.27
	Z5	Arm	El Zanjón	Qtz	qtz, apy	3.59
	24	Arm	El Veneiro	Qtz	qtz, goethite	0.30

Note: Au (ppm) levels determined using fire assay techniques with AAS detection, detection limit 0.01 in data from the present work samples, 0.03 in data from Gómez-Fernández, Vindel, González Clavijo, et al. (2012) samples. Data S3 provides field and laboratory detail. Precise locations are in Data S5. Abbreviations: apy, arsenopyrite; Arm, Armorican quartzite; cpy, chalcopyrite; gn, galena; Man, Manzaneda; ox, oxidized; Pom Mine, Pombriego mine; Pom Vill, Pombriego village; py, pyrite; qtz, quartz.

4. below middle greenschist facies, the overgrowth of euhedral pyrites may partly replace earlier pyrite phases, releasing Au to cracks or rims. Surviving OM is converted to pyrobitumen/graphite, releasing any residual Au to hydrothermal fluids.
5. above middle greenschist facies, pyrite is converted to pyrrhotite, releasing any residual Au and As.

The use of framboidal pyrite as an important palaeoredox proxy in the detection of oceanic anoxic events (Large et al., 2014; Smolarek et al., 2017; Wacey et al., 2014) has provided insights into the earlier processes, focused on the conditions under which pyrite forms in basin sediments. These conditions link S captured from ocean waters and a range of trace elements including As, widely associated with gold in orogenic gold deposits, to an anoxic and euxinic depositional environment (Gregory et al., 2015, 2019; Steadman et al., 2015; Wu et al., 2020) where C from organic material is present. Studies of framboidal pyrite forming in modern sea floor sediments in cores drilled in the South China Sea (Lin et al., 2016), enabled these processes to be studied in detail using NanoSIMS techniques (Gómez-Fernández et al., 2021).

The resulting gold-enriched hydrothermal fluid can transport and re-deposit the Au, subject to the required P–T–x conditions. The content of auriferous hydrothermal fluids generated from black shales rich in carbonaceous OM will impact these P–T–x conditions. They will differ from magmatic fluids and meteoric waters by having a significant diverse volatile content reflecting the presence of C, O, H, S and N in pyritic carbonaceous metasediments from which they are derived, with CH_4 and occasionally other hydrocarbons, including C_2H_6, being determined in fluid inclusions (Gaboury, 2019, 2021). Where aqueous fluid inclusions are absent, hydrocarbons may have been the transporting fluid. The solubility of Au in hydrocarbons has been determined experimentally to be 5–50 times higher than in aqueous solutions and, subject to further research into hydrocarbon-metal complex speciation, this may permit higher levels of Au to be transported and ultimately deposited per unit volume of fluid (Gaboury, 2021).

What data do we need on the black shales? The data presented in Tables 3 and 4 on the host quartz veins reflect the P–T–x conditions applicable during the latest process, the deposition of Au. Regarding earlier processes in the host rock black shales, the relevant data for this paper will be those influencing basin fertility. Under the Large model (Large et al., 2011) the presence of auriferous framboidal pyrites (together with other pyrite textures) in "carbonaceous" host rock is important. Their absence has been reported where TOC of host black shales fall to zero (Smolarek et al., 2017) and hence TOC below detection level would be a contra-indicator for basin fertility for Au. In Harlech, the fluid inclusions in productive phase vein quartz (Table 2) record the presence of both aqueous and, significantly, non-aqueous (CH_4, N_2 and CO_2) fluids, which can form in relatively low P–T conditions. Humic organic material (Wood, 1996) complexes with Au until T > 100°C. Hydrocarbons may survive at temperatures in excess of the normal catagenesis band width

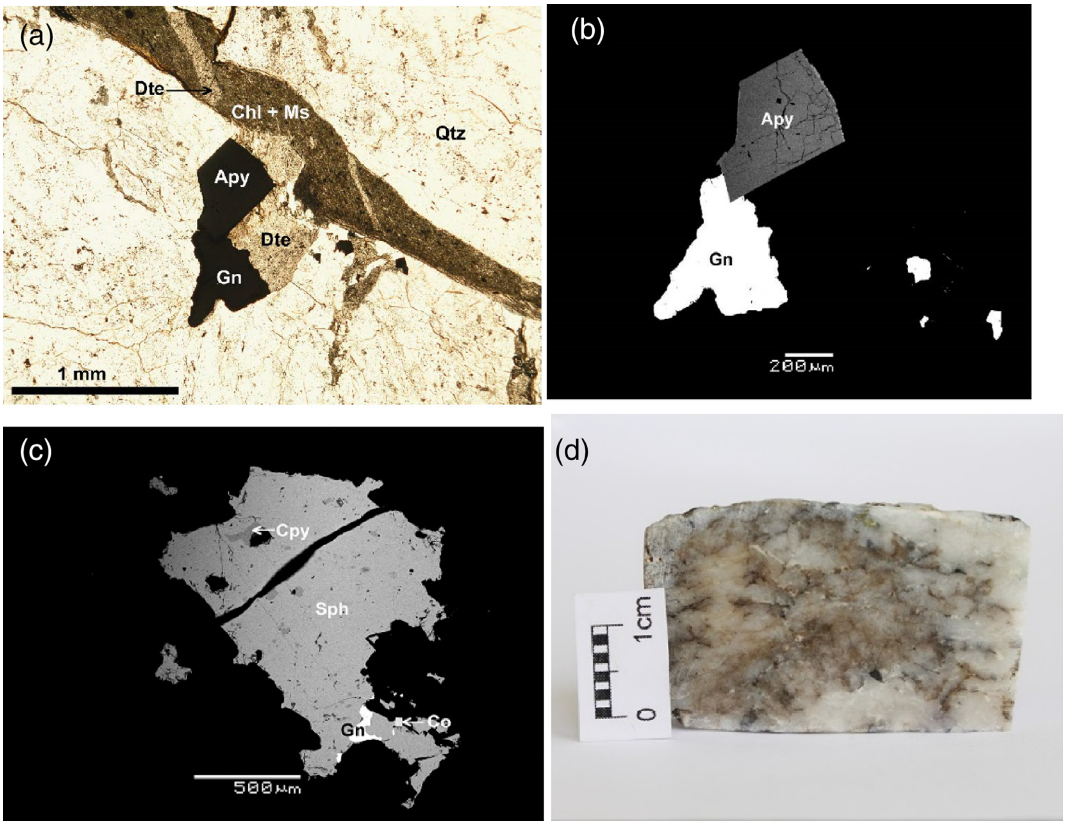

FIGURE 7 Micro- and macrotextures from Harlech (location CCa in Figure 2). (a) Optical microscope (plane-polarized light); (b) and (c) backscattered electron microscope images; (d) macrophotography. Apy, arsenopyrite; Chl, chlorite; Co, cobaltite; Cpy, chalcopyrite; Dte, dolomite; Gn, galena; Ms, muscovite; Qtz, quartz; Sph, sphalerite).

of 60–150°C and hence be available to complex with Au at these temperatures (Gaboury, 2021). Formation of CO_2 and/or CH_4 rich fluids, as a result of oxidation and hydrolysis of organic material under sub-greenschist and lower greenschist conditions, (≈200–300°C) is reported (Křibek et al., 2015). The metamorphic graphite window may open in the lower anchizone (Wang et al., 2012). The pyrite-pyrrhotite transition, important in the metamorphic devolatisation model for orogenic gold (Phillips & Powell, 2010; Tomkins, 2010) is associated with the greenschist–amphibolite transition zone, being complete at 550°C at 3 kbar (Finch & Tomkins, 2017; Zhong et al., 2015) but may commence at sub-greenschist facies and be complete by mid-greenschist facies (Pitcairn et al., 2015). Thus, in summary, the data of interest on the host black shales is that which identifies metamorphic grade (including the difficult area of diagenetic to very low-grade metamorphic rocks), TOC content and the Au content of the Fe sulphides within them.

5.1 | Harlech

In Harlech, the basin sediments are Cambrian turbidites (Figure 2, Data S1). In two horizons, the Clogau Fm and the Dolgellau Fm, black shales are dominant.

5.1.1 | Metamorphic grade

The metamorphic grade (Merriman, 2006) is greenschist (white mica, chlorite ± quartz and albite). However, while detailed work on white mica crystallinity confirms a dominantly epizonal character, there are some indications of very low-grade metamorphism (Table 5). Caution is required in the interpretation of Kübler Index data (KI hereafter) even where the effects of burial during basin fill dominate (Roberts et al., 1989; Roberts et al., 1991; Roberts et al., 1996; Roberts & Merriman, 1985) and tectonic effects (Martínez Poyatos et al., 2001) are only local, as in Harlech. Retrograde metamorphism can introduce complexity (Abad et al., 2010), but this has not occurred in Harlech or Truchas. In both Truchas and Harlech, fluid inclusion data indicates P = ≈2 kbar and hence warnings against use of KI in terranes with pressure gradients other than intermediate (Kisch, 1987) do not apply.

A significant number of these measures of crystallinity are in the anchizone range of 0.42–0.25, where any oil/gas generation is postmature (Laughrey et al., 2011) and incipient or very low-grade metamorphism has commenced (Abad, 2007). During late catagenesis and metagenesis, the non-hydrocarbon gases relevant to Au mineralisation (CO_2, N_2, H_2S) are generated, migrate, may accumulate with CH_4 (Laughrey et al., 2011) and hence be available for storage within fluid inclusions. In the case of N_2, this provides a source for N_2 in

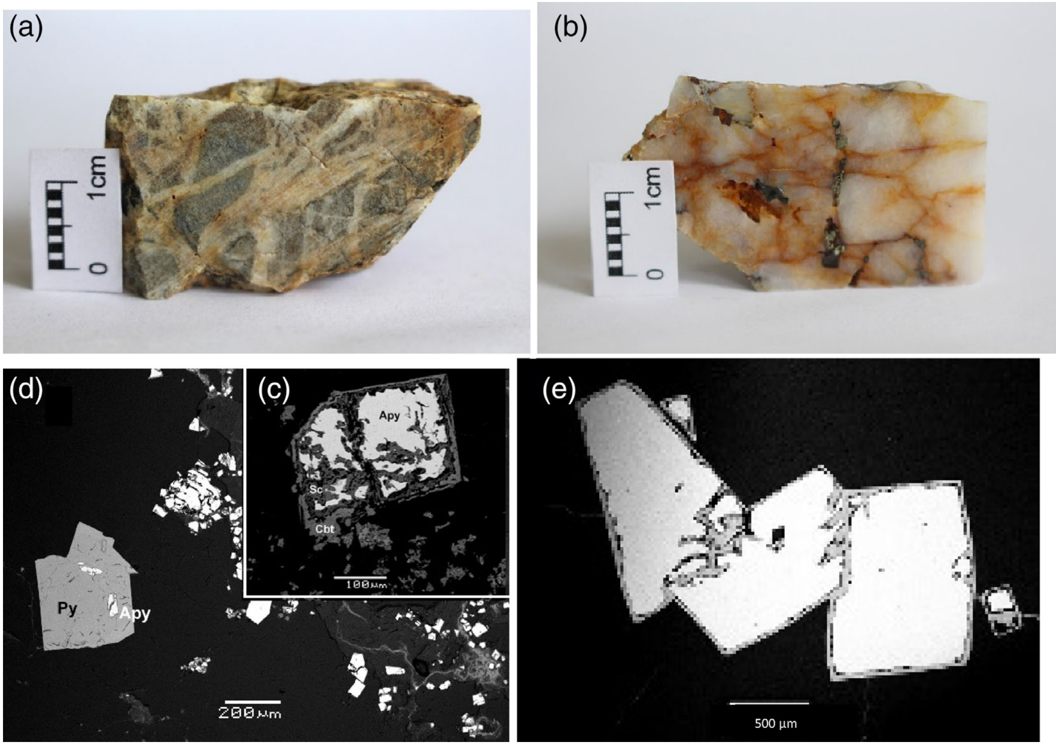

FIGURE 8 Macro- and micro-textures from Manzaneda and Cunas. (a) Manzaneda; (b) Cunas; (c) and (d) BSE images from Manzaneda; e) BSE image of pyrite from Cunas. Apy, arsenopyrite; Chl, chlorite; Gn, galena; Py-pyrite; Sc, scorodite; Sph-sphalerite.

“methanoic” fluid inclusions in productive phase quartz (Table 2) without the wall-rock alteration processes involving NH_4/K ratios discussed later in Section 6.

5.1.2 | Total organic carbon

Data on 31 black shale samples from Harlech, from which 18 determinations of TOC were obtained by pyrolysis, and of C crystallinity, the degree to which organic material has been converted to graphite, are given in Table 6. The highest organic C determined by pyrolysis for samples from the Clogau Fm was 0.69%.

5.2 | Truchas

5.2.1 | Metamorphic grade

Metamorphic grade is reported as within the greenschist facies (Cárdenes et al., 2014, 2018). The world-class slate deposits which characterize Truchas imply KI values in the range 0.15–0.25 (Gómez-Fernández et al., 2009) and are hence epizonal. The isoclinal D1 folding and D2 thrust structures in Truchas (contrasting with the broad open folding at Harlech disturbed only by “meridional” faulting) suggest the tectonic effects of deformation reported from the southern Central Iberian Zone (Martínez Poyatos et al., 2001) will have operated here to increase crystallinity locally, resulting in a range of microfabrics.

(Note: the neutral rock descriptor “black shales” is used in this paper, since in low-grade metapelite basins, the microfabric may range from mudstone to shale to slate (see, for example, Merriman et al., 1990) and use of the term acts as a reminder that it is largely the characteristics of the protolith that are important in determining basin fertility for Au. It is helpful that the black shale protolith may survive in recognizable form over a wide range of time periods (up to 2000 Ma, Merriman, 2005)).

5.2.2 | Total organic carbon

In Truchas and nearby, Ordovician black shales contain sulphides and graphite (Gómez-Fernández et al., 2009; Gómez-Fernández et al., 2019) and show graphitised bright surfaces (Rodríguez Sastre & González Menéndez, 2011). An analysis of dark slate for a roofing slate company product literature determined organic C at 0.24% (Cupa Pizarras, 1998).

5.3 | Fe sulphides found in the black shales in both study areas

Fe sulphides found in the black shales in both study areas exhibit a wide range of textures. In Truchas, they range from framboidal to euhedral pyrite (Figure 9) to pyrrhotite, with relationships with the S_1 tectonic foliation implying pre-kinematic and syn-kinematic growth

TABLE 5 Kübler index values determined for rocks from Harlech

	N	KI Low	KI High	≤0.25 Epizone	High 0.26–0.30 Anchizone	Low 0.31–0.41 Anchizone	≥0.42 Diagenetic
Gritstone	1	0.18		1			
Sandstone	16	0.15	0.24	16			
Siltstone	30	0.14	0.47	25		3	2
Silty mudstone	17	0.15	0.23	12	4	1	
Mudstone	10	0.16	0.36	8	1	1	
Igneous	19	0.17	0.56	9	1	3	6
Total	93			71	6	8	8

Note: Unpublished data from work done by Patrick Daly and Steve Hirons of Birkbeck College (1988–1993). Rocks of sedimentary origin are defined by grain size. Rocks of igneous origin include intrusive and extrusive types, including tuffs.

TABLE 6 Total organic carbon % and carbon crystallinity

	Total organic carbon %					
	N	Min.	Max.	Mean	(σ)	C crystallinity
Clogau Fm (Shale)	11	0.17	0.69	0.38	*(0.18)*	M-H
Dolgellau Fm - black band	4	1.19	3.57	2.33	*(1.21)*	L-M
Dolgellau Fm. (others)	3	0.13	0.51	0.33	*(0.19)*	H

Note: Contains data referenced from BGS MINERALOGY REPORT - WG/AM/77/210R. Permissions courtesy of BGS © UKRI 2022. This unpublished BGS report is referenced as Easterbrook and Basham (1977).
Abbreviations: σ, standard deviation; H, High; L, low; M, medium; Max, maximum value; Mean, mean value; Min, minimum value; N, number of analyses.

(Gómez-Fernández et al., 2009; Gómez-Fernández et al., 2021). In contrast, pentlandite, cobaltite, chalcopyrite, sphalerite, galena, ullmannite and gersdorffite are pre-kinematic but not hydrothermal and reference the trace elements (Ni, Co, Cu, Zn, Sb, As) reported from oceanic pyrite nodules (Gregory et al., 2015, 2019). Scott et al., (2009) caution that formation of framboidal textures is possible during metamorphism at up to anchizonal grade. However, Figure 9 shows features which framboidal pyrite from cored modern sea floor sediments (Lin et al., 2016) exhibit and therefore suggests formation during diagenesis, with subhedral overgrowths forming during low-grade metamorphism.

Studies by EMPA of the different types of pyrite from Truchas (Gómez-Fernández et al., 2019) determined Au levels ranging from 217 ppm (average of 54 analyses) in framboidal pyrite (As level 1999 ppm) to 40–54 ppm Au in euhedral forms, and 54 ppm Au in graphite. While levels of trace elements, including Au, were within detection limits for EMP WDS techniques, the relative levels reported are typical of "gold-only" deposits (Pokrovski et al., 2014). Also As levels were well beyond detection limits and maintained levels at 10–20 times Au across the pyrite types, a common feature of orogenic gold geochemistry. Further detailed studies of the framboidal pyrite (Gómez-Fernández et al. 2021), conducted using LA-ICP-MS and NanoSIMS to map ^{36}S, $^{75}As^{32}S$, ^{75}As, $^{75}As^{34}S$, and ^{197}Au (and perform $\delta^{34}S$ analysis) down to nanoscale allowed 4 types of pyrite to be identified, enabling the identification of high As content nodules at nanoscale, and the growth sequence during diagenesis/early metamorphism. In Harlech, framboidal pyrite has been reported from the Dolgellau Fm and pyrrhotite from the Clogau Fm (Easterbrook & Basham, 1977). Further south in central Wales, framboidal pyrite is associated with Au mineralisation (Annels & Roberts, 1989). However, only euhedral pyrite was present in samples collected from the Clogau Fm for this project.

6 | THE BLACK SHALES AND THE "AMMONIUM" MICAS, ORGANIC MATTER AND THE RELATION WITH FLUID INCLUSIONS IN AURIFEROUS VEIN QUARTZ CONTAINING N_2 AND CH_4 WHERE WALL-ROCK ALTERATION IS SUBSTANTIAL

NH_4 replaces K in "ammonium "micas (e.g., tobelite, $(NH_4,K)Al_2(AlSi_3O_{10})(OH)_2$), found in low temperature reducing environments hosting black shales, where white micas are associated with maturing organic matter (Abad et al., 2007; Wilson et al., 1992). Whole-rock NH_4 contents as high as 2800 ppm have been reported from siliclastic rocks associated with hydrocarbons (Compton et al., 1992; Williams et al., 1995). Black shales remote from mineralisation in Harlech contain 300–1100 ppm NH_4, corresponding to 1000–5500 ppm NH_4 in

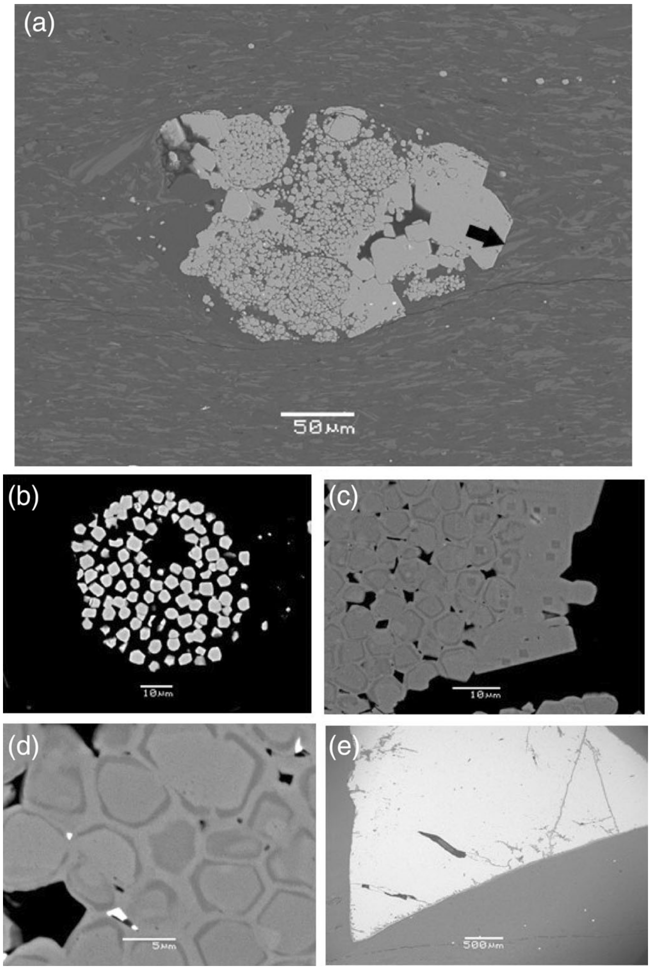

FIGURE 9 Truchas Fe pyrites. (a) Porphyroidal aggregate formed by 3 pre-kinematic framboids within microcrystal aggregates, overgrown by subhedral pyrite cutting the tectonic foliation (S_1) at arrow; (b) framboid (70 μm), crystallites 2–5 μm; (c) and (d) growth textures as pre-kinematic microscrystals are overgrown and the framboid itself acquires an external discontinuous layer of subhedral pyrite; (e) large euhedral pyrite. (Backscattered electron images)

white mica (Bottrell & Miller, 1990). Determination of NH_4 levels in micas present a number of analytical challenges (Abad et al., 2007; Nieto, 2002; Ottolini et al., 2014; Schmidt & Watenphul, 2010). Also, up to upper greenschist facies, it is possible that nitrogen can remain hosted in poorly matured carbonaceous material, rather than micas (Pitcairn et al., 2005). However, the levels in Harlech are of the same order as those determined for metasediments elsewhere (Boyd, 1997; Duit et al., 1986). At the two most prolific mines in the gold belt, the presence of N_2, together with CH_4 (plus minor CO_2) in the "methanoic" fluid inclusions distinguishes auriferous quartz from non-auriferous quartz (Table 2). Wall-rock alteration at the Clogau Mine in Harlech extends to 3 m, involving an inner zone where removal of graphite, inter alia, was reported and an outer zone where, inter alia, K-mica metasomatism occurs (Bottrell, 1986; Gilbey, 1968). Lower NH_4 levels relative to K, reflected in lower whole rock $NH_4/K \times 10^2$ ratios, were determined in the outer alteration zone (Figure 10) than in country rock black shale (Bottrell & Miller, 1990). Thus <0.46–0.04 $NH_4/K \times 10^2$ in the outer alteration zone black shales, 0.93–4.59 $NH_4/K \times 10^2$ in unaltered black shales, implying that, in the outer alteration zone, K had replaced NH_4.

$$K^+ + NH_{4-mica} = NH_3 + H^+ + K_{-mica}.$$

NH_3 released, in the presence of CO_2 from graphite, will produce N_2 and CH_4, in the redox reaction:

$$8NH_3 + 3CO_2 = 4N_2 + 3CH_4 + 6H_2O.$$

As N_2 and CH_4 levels rise, immiscible methanoic fluids are generated into which H_2S partitions and, by removal of S, destabilizes the mobile Au:HS complex leading to deposition of Au in the quartz veins (Brand et al., 1989; Naden & Shepherd, 1989; Shepherd et al., 1991). In Truchas, the host rock is typically a relatively pure quartzite which provides no potential wall-rock source of C or N_2. CH_4 was detected in the fluid inclusions at only one locality (Gomez-Fernández, Vindel, Martín-Crespo et al., 2012), and N_2 not detected. Elsewhere in the Central Iberian Zone, higher levels of gold occur in late-kinematic veins where N_2 levels are enriched (Dee & Roberts, 1993). The source of the N_2 is attributed to interaction of hydrothermal fluids with NH_4 ions in country rock micas and feldspars.

7 | REGIONAL/LOCAL FAULT SYSTEMS AND MINERALISATION

7.1 | Harlech

The Harlech Dome is bounded to the north and south by major regional transpressive shear zones on the NE–SW Caledonoid trend, of which the Bala Fault (Figure 11c) is a member (Howells, 2007). In contrast, within the Dome, the long-lived N-S trending "meridional faults" (Figure 11) are a notable departure from this Caledonoid trend. On a more local scale, both in the gold belt (Figure 2b,c) and in our new study area (Figure 2a), mineralisation is associated with a strong pattern of cross-faults to the ≈N-S "meridional" faults (Figure 11).

The veins were considered to be Devonian in age (Shepherd & Bottrell, 1993), formed at P–T conditions of ≈300°C and 1.8 kbar pressure. However, by analogy with folded, cleaved and boudinised quartz veins located in the Clogau Fm south of Harlech, more recent work suggests that they may be earlier in the deformation history, post the late Tremadoc greenstones, but pre-cleavage (Mason et al., 1999, 2002) and hence preceding the metamorphic hiatus, where P–T conditions were higher at 365°C and 3 kbar.

7.2 | Truchas

In Truchas, significant Au levels (Table 4) were assayed from vein quartz in N-S trending extensional en-echelon fault sets at Llamas de

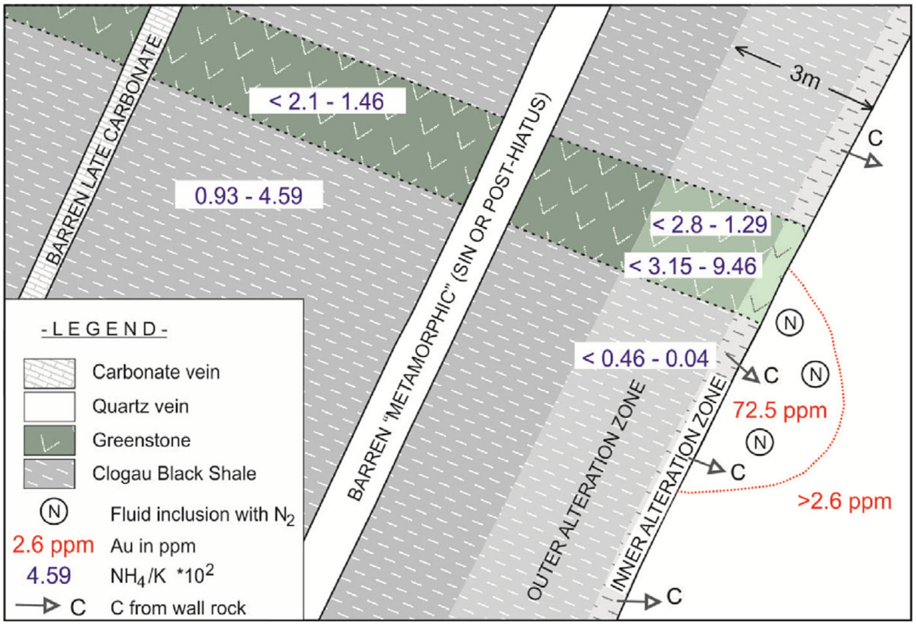

FIGURE 10 Sketch showing spatial relationship between a high grade Au zone (72.5 ppm Au and N_2 in fluid inclusions) in an auriferous quartz vein (>2.6 ppm Au), intensive alteration of the wall-rock black shales, C released from the inner alteration zone, and $NH_4/K \times 10^2$ determinations remote from and within the alteration zone. (after Bottrell & Miller, 1990, Shepherd et al., 1991).

Cabrera (Figures 5a,b) and at Manzaneda (Figures 5c,d, Data S3). At Llamas de Cabrera, these fault sets occur between regional 110° E trending faults. A dextral strike slip component was observed on the regional 110° E fault at Machato (Figure 5a). Applied shear deformation is credible as the process (Kelly et al., 1998; Nicholson & Pollard, 1985; Olson & Pollard, 1991; Rothery, 1988) leading to rotation and associated extension of en-echelon fault sets similar to those seen at Llamas de Cabrera and Manzaneda. In contrast, fault crush zones on the regional 110° E trend (Figure 5e–g) host the significant Au levels at Pombriego.

8 | THE HARLECH AND TRUCHAS “GREENSTONES”

The classification of OGD for both study areas precludes an intrusion-related source, there being no major intrusions. However, minor igneous activity has taken place locally, hosted in the black shales of the Clogau/Maentwrog Fm in Harlech and the Luarca Fm in Truchas. Some “orogenic” gold sources may in fact be polygenetic (Fu et al., 2014; Goldfarb & Groves, 2015; Spence-Jones et al., 2018). Local hydrothermal fluids related to minor intrusions can provide the cryptic aureoles of Merriman and Roberts (2000) and can be active at T > 120–140°C during diagenesis (Haile et al., 2019). Brief descriptions follow and more detail is available in Data S2.

8.1 | The “greenstones” of Harlech

The quartz vein-hosted gold occurrences which led to significant mining activity from 1843 to the 1920s (Hall, 1990) are typically restricted to where the veins intersect the Clogau and Maentwrog Fm of the gold belt, often where altered minor intrusives or “greenstones” also occur (Figure 10 in this paper, Data S2). Alteration is significant, but Allen et al. (1976) were able to detect mineralogy, grain size and texture variation sufficiently to permit classification into dolerites, microdiorites, quartz microdiorites and microtonalites. There are a number of larger greenstone intrusions, which carry porphyry-style Cu-Mo-Au-As mineralisation (Rice & Sharp, 1976). A dominantly calc-alkaline trend is explained by the geotectonic picture (Howells, 2007), with volcanic activity in the North Harlech Basin caused by SE-directed subduction commencing with Late Tremadoc island arc type volcanism, the Rhobell event, (Kokelaar, 1979). The auriferous quartz veins postdate the Rhobell volcanism (Mason et al., 2002), which constrains the role of the greenstones in metallogenesis. A structural, rather than a geochemical role, was considered for the greenstones in localizing Au mineralisation (Platten & Dominy, 2009).

8.2 | The volcanic/subvolcanic rocks of Truchas

Unlike Harlech, no association of these rocks with metallogenesis has been reported from Truchas. New data from our study at Cunas (Table 4, Data S3) confirms the absence of Au and associated elements from quartz veins in the Luarca Fm black shales where volcanic/subvolcanic rocks are particularly plentiful. Previous studies (Brendan Murphy et al., 2008; Suárez et al., 1994) suggest that these Ordovician volcanic rocks represent mantle mafic (±felsic) magmas that were extruded in a marine basin as lavas and volcaniclastic masses. Fernández-Lozano et al. (2016) describe rocks collected from our study area as “deformed altered ignimbrites and tuffs that were reworked in a subaqueous to subaerial environment”. Hence, they contrast strongly with the intrusive signature of the Harlech greenstones. From a metallogenic point of view, new data from our study of the volcanic rocks at Cunas revealed that some volcanic rocks had

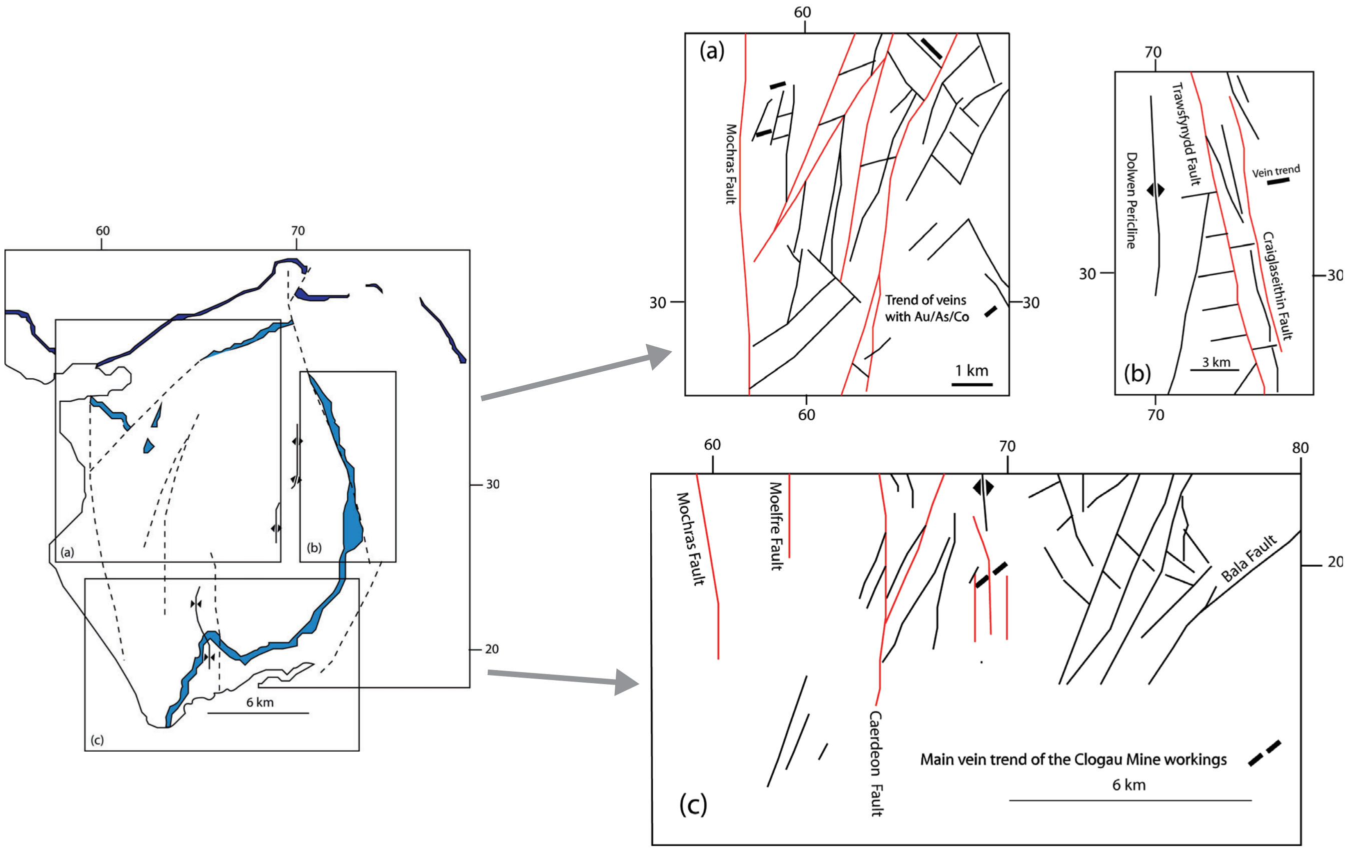

FIGURE 11 Fault patterns and trend of mineralised veins on the Harlech. Dome. The main ≈N-S "meridional" faults are in red. Minor cross-faults host mineralisation. (based on BGS map data, with permissions CP22/019 BGS copyright UKRI 2022. The BGS 1:50000 sheets are named in references (British Geological Survey, 1997, Institute of Geological Sciences, 1978))

experienced late stage carbonate mineralisation (magnesian calcite and ferroan dolomite). In a separate study on the Cunas area (González-Menéndez et al., 2021), we report XCO_2 modelling for the impact of hydrothermal H_2O-CO_2 fluids at temperatures below 350–360°C and fluid XCO_2 between 0.10 and 0.45. Such fluids can be important carriers of Au in other orogenic settings (Phillips & Evans, 2004; Phillips & Powell, 2010). The fluids postdate, or date from the waning stages of, the Variscan low greenschist metamorphic hiatus which affected these rocks at T ≈ 374 ± 6°C, with estimated temperatures of <350–360°C. In the field, the host quartz veins at Cunas are short, narrow and disorderly, both exploiting and cross-cutting the cleavage (Data S3). Textures at the meso and micro scale (Figure 8) demonstrate differences between the auriferous quartz veins at Manzaneda and, on our data, the barren veins of Cunas.

9 | DISCUSSION

For black shale-hosted OGDs, with no magmatic source for the Au and associated trace elements (in particular As), the levels of these elements captured in basin sediments provide an indication of basin fertility. As described by Large et al. (2011) for Carlin-type and some orogenic gold deposits, gold captured in basin muds/organic matter and incorporated in framboidal pyrite would be released into hydrothermal fluids as a consequence of the evolution of framboidal pyrites to euhedral forms and of organic matter to graphite, during diagenesis and low grade metamorphism. Large et al. (2011) propose 250 ppb Au in diagenetic pyrite as an indicative threshold level for potential source rocks. Sack et al. (2018) report framboidal pyrite contents of 670 ppb Au and 1223 ppm As as a proxy for gold fertility in the Selwyn basin area, Yukon. The levels of 217 ppm Au and 1999 ppm As in framboidal pyrite from Truchas, together with the other data reported in Gómez-Fernández et al. (2019), Gómez-Fernández et al. (2021), are therefore significant. For a large number of OGDs, the metamorphic model, with pervasive mobilization of fluids being produced in the greenschist/amphibolite transition zone, is proposed (Phillips & Powell, 2010; Tomkins, 2010). This transition zone is crucial to scavenging of Au and associated elements during devolatization of chlorite (Zhong et al., 2015). Basin fertility in these conditions can be estimated by mass balance calculations, based on sampling/analysis of host rock for Au/other trace elements (Pitcairn et al., 2006; Pitcairn et al., 2015; Pitcairn et al., 2017; Pitcairn et al., 2021) yielding whole-rock levels as low as 0.21–4.2 ppb Au in unmetamorphosed/low grade protolith. However, metamorphic grade of the host rocks in Harlech and Truchas does not exceed greenschist facies, as is the case for many black shale-hosted OGDs (Bierlein & Maher, 2001). Thus, such Au scavenging could not have occurred at the observed crustal levels of the studied sites (Clogau Fm, Luarca Fm and Armorican Quartzite Fm). Wu et al. (2019) report that gold and other metals contained in pyrites can be released into hydrothermal fluids by dissolution and reprecipitation processes stimulated by fault valve variations in P at much lower temperatures. Our detailed work on the framboidal pyrite from Truchas (Gómez-Fernández et al., 2021) concludes that diagenetic to low-grade metamorphic conditions applied during Au capture and release. In Truchas, P–T conditions determined for Au deposition in the quartz veins range 180–310°C (Gomez-Fernández, Vindel, Martín-Crespo et al., 2012), sub-greenschist facies, and lower than the mesozonal range (300–475°C and 6–12 km) of Groves et al. (1998). This accords with regional studies in NW Iberia (Boiron et al., 1996; Noronha et al., 2000) which report P–T conditions implying <3 km depth and <300°C at deposition for auriferous quartz. This follows an earlier phase of non-auriferous quartz deposition (containing arsenopyrite and pyrite) where P–T conditions during orogenic uplift and tectonic reactivation imply 3–9 km depth and 300–450°C. Useful further insights into P–T conditions of very low-grade metamorphism of C-rich siliclastics which contain framboidal pyrite are provided by well studies. At a maximum burial depth of >8 km (Laughrey et al., 2011), temperatures range over 200–250°C and organic metagenesis continues within an anchizonal regime. At 7 km, Wang et al. (2012) report persistence of the anchizone and temperatures range 200–270°C, with a 348°C outlier. Taken together, these P–T conditions are closer to those in Carlin-type gold deposits (Berger et al., 2014; Cline et al., 2005; Hofstra & Cline, 2000; Radke & S., 1985) than to those in higher grade orogenic belts (Finch & Tomkins, 2017; Tomkins, 2013) and is supportive of the model described by Large et al. (2011) for Carlin-type and some orogenic gold deposits.

9.1 | Structural controls for Au deposition

New observations at Llamas de Cabrera and Manzaneda complement the metallogenic-structural model of Gómez-Fernández et al. (2005), (Gómez-Fernández, Vindel, Martín-Crespo, et al., 2012). According to this model, most of the vein gold occurrences reported from Llamas de Cabrera occur in N-S extensional fractures, in a closely-spaced cluster between two 110° E faults. Most of these veins occur in the Armorican Quartzite, but near the contact with the overlying Luarca Fm. Significant levels also occur localized to faults on the regional 110° E trend at Pombriego. In Harlech (Figure 11), the "meridional" fault-hosted quartz veins did not contain Au at any of the localities studied. Instead auriferous veins were located on cross-faults from the "meridional" faults. Geochemical and structural models may of course co-exist, and may co-exist on different scales. Bierlein et al. (2001), combining structural and geochemical models with data from metasedimentary-hosted gold deposits in Victoria, Australia, concluded that, at the deposit level, structures are the key control, while at a local level, redox controlled precipitation of Au could occur as auriferous hydrothermal fluids encountered "carbonaceous" beds.

9.2 | Wall-rock fluid interaction and geochemical controls over Au transportation and deposition: The role of NH_4 and C

Hydrothermal systems are efficient in recycling NH_4 (Stüeken et al., 2021). The significance of NH_4 in gold mineralisation has been discussed for deposits in the Carlin trend, vein-type epithermal precious metal deposits, Witwatersrand reefs, a wide range of OGDs, the auriferous orogenic belt of South Island, New Zealand and the contact aureole of intrusion-related gold systems (Fu et al., 2014; Jia, 2002; Kydd & Levinson, 1986; Meyer & Ridgway, 1991; Pitcairn et al., 2005; Ridgway et al., 1990) with general agreement that nitrogen levels and isotopic values for mica and whole rock samples reflect inheritance from sedimentary kerogen. For Harlech, the role for NH_3 ions derived from K/NH_4 replacement in white mica is plausible. In the presence of CO_2, NH_3 participates in the generation of an immiscible "methanoic" phase rich in N_2 and CH_4 (Bottrell & Miller, 1990; Shepherd et al., 1991), into which H_2S partitions, destabilizing gold bisulphide complexes and causing deposition of Au. Bottrell and Miller (1990) note that wall-rock shales are severely depleted in NH_4 only in the zones of most intense alteration. This may account for low Au levels assayed in our new study area in Harlech. The null hypothesis would be that if no wall-rock alteration took place where veins cut the Clogau Fm or Maentwrog metapelites, no C or N_2 could have been sourced. No wall-rock alteration was observed in our new study area (other than localized intense brecciation/alteration at one location, Letty'r-Fwyalch [Data S4B], where none of the early phase or productive Au phase minerals are present, apart from pyrite). The low Au levels assayed from samples from our new study area in Harlech are therefore compatible with this null hypothesis.

In the Harlech model described above, CO_2 participates and a wall-rock source of C is proposed. A contrarian view is provided (Hu et al., 2017) which suggests that most carbonaceous material is derived from ore fluids, rather than an organic source in altered wall-rocks. In the Hu et al., 2017 model, carbonaceous material and pyrite are co-deposited from ore fluids, so reducing H_2S, destabilizing gold bisulphide complexes and precipitating gold. Their data (in their Figure 2) show non-carbonate carbon levels are clustered at similar levels to those reported in this paper. C, regardless of source, clearly has a role in both models. However, the Harlech model explains the presence of N_2 in the "methanoic" fluid inclusions. In Harlech, gold-bearing quartz veins precede the metamorphic hiatus (Mason et al., 1999). They could reflect an environment where hydrothermal activity and vein emplacement on a local (not pervasive) scale occurred much earlier in basin history, perhaps not long after the transition from diagenesis to metamorphic conditions, a very different transition to that proposed by the metamorphic devolatilisation model, where chemical/mineralogical changes are pervasive. While N_2 is present in the Harlech "methanoic" fluid inclusions, H_2 is absent. This contrasts with orogenic gold mineralisation in the Otago Schist, New Zealand where H_2 and N_2 often coexist, with $H_2 > N_2$, the greenschist/amphibolite transition is present and the hydrocarbon gases (e.g., CH_4, C_2H_6) created during maturation of carbonaceous

OM in earlier basin history will degrade at much higher temperatures after basin inversion to yield H_2 (Gaboury et al., 2021). But the greenschist/amphibolite transition is not reached in Harlech, with the Kübler Index values (Table 5) including some low anchizone levels, post mature from a hydrocarbon gas generation perspective, but some distance from conditions which would generate H_2 from their breakdown. A range of 315–700°C at 1 atmosphere was determined experimentally for $CH_4 > C + 2H_2$ (Gaboury et al., 2021). The bonanzas such as those at Clogau and Gwynfynydd may simply reflect the local presence of exceptional levels of C, and also NH_4 in the "ammonium" minerals in the host wall-rocks.

9.3 | A proposed model for the Truchas mineralisation

Gómez-Fernández et al. (2019), in the Truchas Syncline, advocate for a local gold source from a black shale protolith subjected to lower P–T conditions than those of the greenschist/amphibolite transition zone. The complete model, from source to depositional environment is summarized in Figure 12.

The gold would have been captured in the diagenetic pyrites and in the organic matter of the black shales of the Luarca Fm. The similarity of the S^{34} values for the two As–Fe ore stages and for pyrites from the Luarca Fm are supportive of an origin within basin sediments in Truchas. In accordance with the process described by Large et al. (2011) for Carlin-type and orogenic gold deposits, part of this gold would have been released into the hydrothermal fluids as a consequence of the evolution of framboidal pyrites to euhedral forms and of organic matter to graphite, during diagenesis and the metamorphism associated with the Variscan orogeny. Subsequently, it would have been precipitated in extensional zones developed mainly in the adjacent competent rock, the Armorican quartzite. Regarding the timing of mobilization and deposition, the D1 event (approx. 350 Ma, Rubio-Pascual et al., 2013) is the peak of high P metamorphism. The thermal peak, when Au could have been more easily mobilized, occurred at approx. 330–310 Ma in the Iberian NW Variscan basement (Cuesta & Gallastegui, 2004; González-Menéndez et al., 2019; Rubio-Pascual et al., 2013). This event was mainly extensional towards the inner part of the orogen; most of the Variscan granitoid magmas formed and were emplaced at this time, with accommodative extension. Thus we have both high T metamorphism (thermal peak) and extensional conditions during approx. 330–310 Ma in this part of NW Spain. This could link the mobilization of Au, in the lower/middle crust by metamorphic fluids, and its deposition in upper crustal, local, extensional structures. Supportive regional studies of Au mineralisation in NW Iberia (Boiron et al., 1996; Noronha et al., 2000) established that the Variscan granites were not a source for Au, but were a heat source driving successive periods of fluid circulation during uplift of basement/intrusion of the granites and that quartz-sealed faults tapped shallow and deep-seated reservoirs (Boiron et al., 2003).

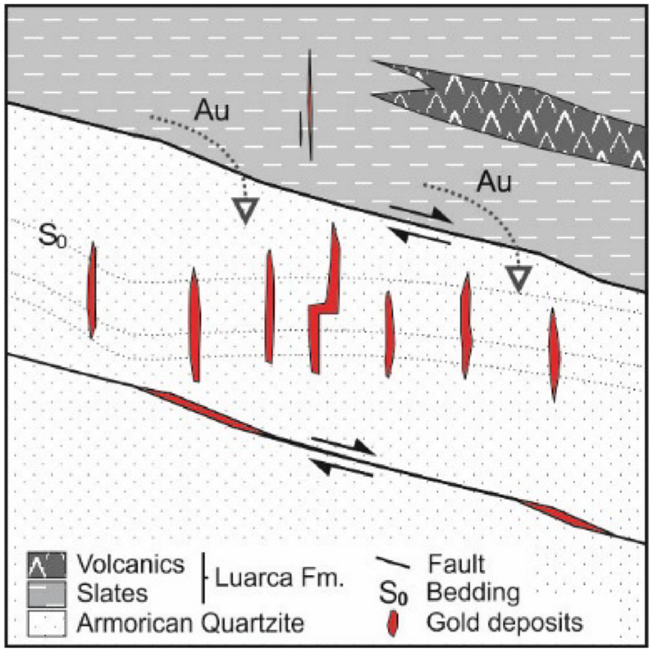

FIGURE 12 Diagram modelling the migration of Au from the pyrites of the Luarca Fm. to extensional zones developed mostly in the Armorican quartzite in response to strike-slip faults

9.4 | Assignment to deposit typology

Mortensen et al. (2022) propose, based inter alia on tectonic setting, lithological siting, and characteristics of the mineralisation in each subtype, the division of the Phanerozoic OGDs into four sub-types: crustal-scale fault (CSF) subtype, sediment-hosted orogenic gold (SHOG) subtype, forearc (FA) subtype and syn- to late-tectonic, dispersed (SLTD) subtype. Caution is advised, as complex orogenic belts may host two or more contemporaneous subtypes and in any case subtypes may be transitional. The Truchas deposits can be assigned to the SLTD subtype whose main characteristics are: (a) simple fissure veins, less abundant fault veins, (b) widely distributed vein arrays typically not associated with major structures (the Truchas faults do not exceed a few kilometres in length, so they cannot be considered major strike slip faults), (c) late stage veins usually localized in extensional fracture arrays in brittle crust and (d) strong lithological control (local sources). Additional characteristics of economic significance are that they are likely to be small, locally high grade but associated with significant alluvial gold deposits, as in Truchas. Assigning Harlech to one of the Mortensen et al. (2022) subtypes is more problematic. The tectonic setting is close to the Iapetus Suture, where oblique convergence between Avalonia with Laurentia provides the mechanism for transpression to occur. The Harlech Dome is a N-S orientated complex anticline, lying between major NE trending terrane-bounding fault zones, along which sinistral movement took place (Howells, 2007). Thus, the key feature of crustal-scale fault (CSF) subtype, that they occur within and adjacent to crustal scale transpressive fault zones, including terrane bounding structures, is met. Mortensen et al., (op.cit.) report that the veins are commonly ribbon-banded, a feature of the most productive veins in Harlech (Platten & Dominy, 2009) and there is an association of greenstones with the productive veins. However, the key association with metapelites within a thick turbidite sequence in Harlech would suggest the SHOG mineralisation subtype, of which the Meguma terrane is an example (Kontak et al., 1990; Ryan & Smith, 1998). In that terrane, gold-bearing lenses of disseminated pyrite and arsenopyrite in sediments occur in addition to epithermal deposits, suggesting Au capture in basin sediments before re-mobilization to the economically important mineral sites. This two-stage process has features of that proposed above for Truchas in Figure 12. Vein-style SHOG deposits share the characteristic of being small/mostly sub-economic with the SLTD subtype, unless local Au-rich sources exist.

10 | CONCLUSIONS

The Harlech Dome in Wales and the Truchas Syncline in Spain provide examples of the occurrence of auriferous quartz veins in Palaeozoic metasediments which include black shales, an orogenic gold association with a global reach. The mineral paragenesis in both areas reflect the mesozonal orogenic gold-only model (Groves et al., 1998; Pokrovski et al., 2014), with an early arsenopyrite/pyrite phase and a later base-metal sulphide dominated phase hosting Au.

In both areas, gold deposition from hydrothermal fluids occurs in veins localized to extensional cross-fault systems, which are associated with larger faults in Harlech which extend for a maximum of ≈20 km, and which extend to no more than 3 or 4 km in length in Truchas, but are not crustal scale transpressive fault zones. Thus, favourable conditions for mineralisation appear to be related primarily to local fault-related decompression. Nevertheless, the data presented in this paper is in part supportive of the hypothesis that the gold mineralisation in Harlech is facilitated by chemical interaction of hydrothermal fluids with wall-rocks (which are carbonaceous and contain minerals in which NH_4 ions, captured from the sedimentary environment, replace K). Accordingly, the role of the local metapelite composition might be more important in the case of Harlech than in the case of Truchas.

Turning to the origin of the mineralizing fluids and the gold, the model of metamorphic devolatilization is noted (op.cit.). This model is contrasted, at least in part, with the model of Gómez-Fernández et al. (2019), according to which, in the Truchas Syncline, the origin of the gold would be in the biogenic pyrites and the organic matter of the Luarca Fm. During diagenesis and low-grade metamorphism, some of this gold and other metals would have been released to the metamorphic/hydrothermal fluids at modest T conditions, to be subsequently deposited in extensional areas, developed mainly in adjacent competent rocks.

The deposits of Truchas are assigned to the SLDT subtype (Mortensen et al., 2022). The assignment of the Harlech deposits to one of the subtypes of Mortensen et al. (2022) is more complex, and while a case can be made that the CSF subtype applies, with greater economic potential, the argument for the quartz-vein SHOG subtype is more compelling. The exploration strategy for the favoured subtypes (vein style SHOG and SLDT) relies upon identifying local favourable structural features and, crucially, where Au-enriched source areas are present in local basin metasediments.

ACKNOWLEDGEMENTS

This project was partially funded by Project 0284_SIIMET_3_E, belonging to the INTERREG V-A Spain-Portugal Cooperation Programme (2014–2020). The support of Gavin Birkenheger of GreenOre Gold is gratefully acknowledged. J.K. Cunningham acknowledges the valuable assistance given by Hank Sombroek, Pat Daly, Maz Iqbal, Steve Hirons, Dick Merriman, David Kossoff and Gina Easterbrook in UK and Javier Fernández-Lozano in Spain. The manuscript has been considerably improved by the comments of the reviewers, Eva Stüeken, Jim Mortensen, Michael Gadd and Jeff Steadman. We thank Professor Li Tang (Editor) for his support.

AUTHOR CONTRIBUTION

Each author contributed to the conception and design of the paper, as well as acquisition and interpretation of the data, analysis of the results and to the writing of the manuscript.

CONFLICT OF INTEREST

The authors declare that they have no financial interests or personal relationships that could influence the work reported in this paper.

DATA AVAILABILITY STATEMENT

The data that support the findings of this study are available from the corresponding author upon reasonable request.

ORCID

John Keiller Cunningham https://orcid.org/0000-0001-7527-1444

REFERENCES

Abad, I. (2007). Physical meaning and applications of the illite Kübler index: measuring reaction progress in low-grade metamorphism. In F. Nieto & J. Jiménez-Millán (Eds.), *Diagenesis and low-temperature metamorphism. Theory, Methods and Regional Aspects [meeting Held on September 11th–14th in Jaén (Spain)] Volume 3 of Seminarios de la Sociedad Española de Mineralogía* (pp. 53–64). Seminarios.

Abad, I., Livi, K., Nieto, F., Árkai, P., & Judik, K. (2007). Analysis of ammonium in micas by electron energy-loss spectroscopy. In F. Nieto & J. Jiménez-Millán (Eds.), *Diagenesis and low-temperature metamorphism: Theory, Methods and Regional Aspects [meeting held on September 11th–14th in Jaén (Spain)] Volume 3 of Seminarios de la Sociedad Española de Mineralogía* (p. 99). Seminarios.

Abad, I., Murphy, J. B., Nieto, F., & Gutierrez-Alonso, G. (2010). Diagenesis to metamorphism transition in an episutural basin; the late Paleozoic St. Mary's basin, Nova Scotia, Canada. *Canadian Journal of Earth Sciences*, *47*(2), 121–135.

Allen, P. M., Cooper, D. C., Fuge, R., & Rea, W. J. (1976). Geochemistry and relationships to mineralisation of some igneous rocks from the Harlech dome, Harlech. *Transactions of the Institution of Mining and Metallurgy, (Section B: Applied Earth Science)*, *85B*, 100–108.

Annels, A. E., & Roberts, D. E. (1989). Turbidite-hosted gold mineralisation at the Dolaucothi gold mines, Dyfed, Wales, United Kingdom. *Economic Geology*, *84*, 1293–1314.

Berger, V.I., Mosier, D.L., Bliss, J.D., & Moring, B.C. (2014). Sediment-hosted gold deposits of the world—Database and grade and tonnage models. US Geological Survey Open-File Report. 1074.

Bierlein, F. P., Cartwright, I., & McKnight, S. (2001). The role of carbonaceous 'indicator' slates in the genesis of lode gold mineralization in the western Lachlan Orogen, Victoria, southestern Australia. *Economic Geology*, *96*, 431–451.

Bierlein, F. P., & Maher, S. (2001). Orogenic disseminated gold in Phanerozoic fold belt examples from Victoria, Australia and elsewhere. *Ore Geology Reviews*, *18*, 113–148.

Boiron, M.-C., Cathelineau, M., Banks, D. A., Fourcade, S., & Vallance, J. (2003). Mixing of metamorphic and surficial fluids during the uplift of the Hercynian upper crust: Consequences for gold deposition. *Chemical Geology*, *194*(1–3), 119–141.

Boiron, M.-C., Cathelineau, M., Banks, D. A., Yardley, B. W. D., Noronha, F., & Miller, M. F. (1996). P-T-X conditions of late Hercynian fluid penetration and the origin of granite-hosted gold quartz veins in northwestern Iberia: A multidisciplinary study of fluid inclusions and their chemistry. *Geochimica et Cosmochimica Acta*, *60*(1), 43–45.

Bottrell, S.H. (1986). *The origin of the gold mineralization of the Dolgellau region, North Harlech: The chemistry and role of fluids*. Unpublished PhD thesis, University of East Anglia.

Bottrell, S. H., & Miller, M. F. (1990). The geochemical behaviour of nitrogen compounds during the formation of black shale-hosted quartz-vein gold deposits, North Harlech. *Applied Geochemistry*, *5*, 5289–5296.

Bottrell, S. H., Shepherd, T. J., Yardley, B. W. D., & Dubessy, J. (1988). A fluid inclusion model for the genesis of the ores of the Dolgellau Gold Belt, North Harlech. *Journal of the Geological Society of London*, *145*, 139–145.

Boyd, S. R. (1997). Determination of the ammonium content of potassic rocks and minerals by capacitance manometry - a prelude to the calibration of FTIR microscopes. *Chemical Geology*, *137*, 57–66.

Brand, N. W., Bottrell, S. H., & Miller, M. F. (1989). Concentrations of reduced Sulphur in inclusion fluids associated with black shale-hosted quartz vein gold deposits: Implications for mechanisms of transport and deposition of gold and a possible exploration tool. *Applied Geochemistry*, *4*, 483–491.

Brendan Murphy, J., Gutiérrez-Alonso, G., Fernández-Suárez, J., & Braid, J. A. (2008). Probing crustal and mantle lithosphere origin through Ordovician volcanic rocks along the Iberian passive margin of Gondwana. *Tectonophysics*, *461*, 166–180.

British Geological Survey. (1997). *Snowdon, sheet 119, 1:50,000 series* (Solid ed.). Southampton.

Cárdenes, V., Merinero, R., López-Mungira, A., Rubio-Ordoñez, Á., Pitcairn, I. K., & Cnudde, V. (2018). Size evolution of micropyrite from diagenesis to low-grade metamorphism. *Geological Society, London, Special Publications*, *478*, 137–144. https://doi.org/10.1144/SP478.2

Cárdenes, V., Rubio-Ordoñez, A., Wichert, J., Cnudde, J. P., & Cnudde, V. (2014). Petrography of roofing slates. *Earth Science Reviews*, *138*, 435–453.

Carpi, A., & Egger, A. (2008). Comparison in Scientific Research. https://www.visionlearning.com/en/library/Process-of-Science/49/Comparison-in-Scientific-Research/152

Cline, J. S., Hofstra, A. H., Muntean, J. L., Tosdal, R. M., & Hickey, K. A. (2005). Carlin-type gold deposits in Nevada: Critical geologic characteristics and viable models. In *Economic Geology* 100th Anniversary Volume (pp. 451–484). Society of Economic Geologist, Inc.

Compton, J. S., Williams, L. W., & Ferrell, R. E. (1992). Mineralization of organogenic ammonium in the Monterey formation, Santa Maria and San Joaquin basins, California, USA. *Geochimica et Cosmochimica Acta*, *56*, 1979–1991.

Cox, S. F., Sun, S. S., Etheridge, M. A., Wall, V. J., & Potter, T. F. (1995). Structural and geochemical controls on the development of turbidite-hosted gold quartz vein deposits, wattle gully mine, Central Victoria, Australia. *Economic Geology*, *90*, 1722–1746.

Cuesta, A., & Gallastegui, G. (2004). Magmatismo de la Zona Centro ibérica: Galicia occidental. In J. A. Vera (Ed.), *Geología de España* (pp. 96–100). SGE-IGME.

Dee, S. J., & Roberts, S. (1993). Late-kinematic gold mineralisation during regional uplift and the role of nitrogen: An example from the La Codosera area, W Spain. *Mineralogical Magazine*, *57*, 437–450.

Duit, W., Jansen, J. B. H., van Bremen, A., & Bos, A. (1986). Ammonium micas in metamorphic rocks as exemplified by dome de l'Agout (France). *American Journal of Science*, *286*, 702–732.

Easterbrook, G.D., & Basham, I.R. (1977). *Investigations into the causes of electromagnetic anomalies in Cambrian and Ordovician sediments in the Harlech Dome*. Report No. 210, Mineralogy Unit, Institute of Geological Sciences, Geochemical Division, Keyworth, Nottingham, UK.

Fernández, F. J. (2001). Características estratigráficas y estructurales del margen noroccidental del sinclinorio de Truchas: geología aplicada a la prospección y explotación de pizarras para techar. *Revista. Sociedad Geologica de España*, *14*(3–4), 161–173.

Fernández, F. J., Aller, J., & Bastida, F. (2007). Kinematics of a kilometric recumbent fold: The Caurel Synform (Iberian massif, NW Spain). *Journal of Structural Geology*, *29*(10), 1650–1664.

Fernández-Lozano, J., Gutiérrez-Alonso, G., & Fernández-Morán, M. A. (2015). Using airborne LiDAR sensing technology and aerial orthoimages to unravel Roman water supply systems and gold works in NW Spain (Eria valley, León). *Journal of Archaeological Science*, *53*, 356–373.

Fernández-Lozano, J., Pastor-Galán, D., Gutiérrez-Alonso, G., & Franco, P. (2016). New kinematic constraints on the Cantabrian orocline: A paleomagnetic study from the Peñalba and Truchas synclines, NW Spain. *Tectonophysics*, *681*, 195–208.

Finch, E. G., & Tomkins, A. G. (2017). Pyrite-pyrrhotite stability in a metamorphic aureole: Implications for orogenic gold genesis. *Economic Geology*, *112*(3), 661–674.

Fu, B., Mernagh, T. P., Fairmaid, A. M., Phillips, D., & Kendrick, M. A. (2014). CH_4-N_2 in the Maldon gold deposit, Central Victoria, Australia. *Ore Geology Reviews*, *58*, 225–237.

Gaboury, D. (2019). Parameters for the formation of orogenic gold deposits. *Applied Earth Science, Transactions of the Insitute of Mining and Metallurgy, Section B*, *128*(3), 124–133.

Gaboury, D. (2021). The neglected involvement of organic matter in forming large and rich hydrothermal orogenic gold deposits. *Geosciences*, *2021*(11), 344. https://doi.org/10.3390/geosciences11080344

Gaboury, D., MacKenzie, D., & Craw, D. (2021). Fluid volatile composition associated with orogenic gold mineralization, Otago schist, New Zealand: Implications of H_2 and C_2H_6 for fluid evolution and gold source. *Ore Geology Reviews*, *133*, 104086.

Gilbey, J.W. (1968). *The mineralogy, paragenesis and structure of the ores of the Dolgellau Gold Belt, Merionethshire, and associated wall rock alteration*. Unpublished PhD thesis, University of London.

Goldfarb, R. J., & Groves, D. I. (2015). Orogenic gold: Common or evolving fluid and metal sources through time. *Lithos*, *233*, 2–26.

Gómez-Fernández, F., Castano, M. A., Bauluz, B., & Ward, C. R. (2009). Optical microscope and SEM evaluation of roofing slate fissility and durability. *Materiales de Construcción*, *59*(296), 91–104. https://doi.org/10.3989/mc.2009.44007

Gómez-Fernández, F., Cunningham, J. K., Caldevilla, P., Herrero-Hernández, A., & Beard, A. D. (2019). The source of Au and S of the orogenic gold deposits in the llamas de Cabrera district (Iberian

Variscan massif). In *Life with ore deposits on earth* (Vol. 2, pp. 842–845). 15th SGA biennial meeting 2019.

Gómez-Fernández, F., Cunningham, J. K., Caldevilla, P., Herrero-Hernández, A., & Beard, A. D. (2021). Microscopic and NanoSIMS characterization of black shale-hosted pre-kinematic pyrites: Possible gold source of the orogenic gold deposits in the Truchas syncline (Variscan Iberian massif**)**. *Ore Geology Reviews*, *138*(7), 104344.

Gómez-Fernández, F., Matías, R., Méndez, A. J., & Cifuentes, J. (2005). Estudio preliminar de las mineralizaciones de la mina de oro romana de Llamas de Cabrera (León, NO de España*)*. *Estudios Geológicos*, *61*, 111–119.

Gómez-Fernández, F., Vindel, E., González Clavijo, E., Martín-Crespo, T., & Sánchez, V. (2012). Lithogeochemistry of the Llamas de Cabrera gold district (Northwest Spain): metallogenetic implications. In M. Quinta-Ferreira, M. T. Barata, F. C. Lopes, A. I. Andrade, M. H. Henriques, R. Pena dos Reis, & E. Ivo Alves (Eds.), *Para desenvolver a terra: Memorias e noticias de geociencias no espaco lusofono* (pp. 483–492). Imprensa da Universidade de Coimbra.

Gómez-Fernández, F., Vindel, E., Martín-Crespo, T., Sánchez, V., González Clavijo, E., & Matías, R. (2012). The llamas de Cabrera gold district, a new discovery in the Variscan basement of Northwest Spain: A fluid inclusion and stable isotope study. *Ore Geology Reviews*, *46*, 68–82.

González-Menéndez, L., Gallastegui, G., Cuesta, A., González Cuadra, P., & Rubio-Ordóñez, A. (2019). Granitos y rocas metamórficas del Oeste de Galicia (costa occidental gallega - Isla de Ons). In *6ª Reunión del Grupo Ibérico de Petrología, Geoquímica y Geocronología* (p. 92). España.

González-Menéndez, L., Gómez-Fernández, F., Cunningham, J. K., Menéndez, S., Caldevilla, P., Gallastegui, G., & Cuesta, A. (2021). Ordovician volcanic rocks record rifting, Variscan metamorphism and gold mineralization processes (Truchas Syncline, NW Iberia, Spain). *Journal of Iberian Geology*, *47*, 387–409.

Gregory, D. D., Large, R. R., Halpin, J. A., Baturina, E. L., Lyons, T. W., Wu, S., Danyushevsky, L. V., Sack, P. J., Chappaz, A., Maslennikov, V. V., & Bull, S. W. (2015). Trace element content of sedimentary pyrite in black shales. *Economic Geology*, *110*(6), 1389–1410.

Gregory, D. D., Mukherjee, I., Olson, S. L., Large, R. R., Danyushevsky, L. V., Stepanov, A. S., Avila, J. N., Cliff, J., Ireland, T. R., Raiswell, R., Olin, P. H., Maslennikov, V. V., & Lyons, T. W. (2019). The formation mechanisms of sedimentary pyrite nodules determined by trace element and sulfur isotope microanalysis. *Geochimica et Cosmochimica Acta*, *259*, 53–68.

Groves, D. I., Goldfarb, R. J., Gebre-Mariam, M., Hagemann, S. G., & Robert, F. (1998). Orogenic gold deposits: A proposed classification in the context of their crustal distribution and relationship to other gold deposit types. *Ore Geology Reviews*, *13*, 7–27.

Haile, B. G., Czarniecka, U., Xi, K., Smyrak-Sikora, A., Jahren, J., Braathen, A., & Hellevang, H. (2019). Hydrothermally induced diagenesis: Evidence from shallow marine-deltaic sediments, Wilhelmøya, Svalbard. *Geoscience Frontiers*, *10*(2), 629–649.

Hall, G. W. (1990). *The gold mines of Merioneth* (2nd ed.). Griffin Publications.

Herail, G. (1984). *Géomorfologie et gitologie de l'or détritique*. Piédmont et bassins intramontagneux du Nord-Ouest de l´Espagne. Centre National de la Recherche Scientifique (CNRS), Paris.

Hofstra, A. H., & Cline, J. S. (2000). Characteristics and models for Carlin-type gold deposits. *SEG Reviews*, *13*, 163–220.

Howells, M. F. (2007). *British regional geology: Harlech*. British Geological Survey.

Hu, S. Y., Evans, K., Craw, D., Rempel, K., & Grice, K. (2017). Resolving the role of carbonaceous material in gold precipitation in metasediment-hosted orogenic gold deposit. *Geology*, *45*(2), 167–170.

Huyck, H. L. O. (1990). Proposed definition of "black shale" and "metalliferous black shale" for IGCP #254. In *Book of abstracts 8th IAGOD symposium* (pp. A183–A184). Geological Survey of Canada.

Institute of Geological Sciences. (1978). Harlech, sheet 135 and part of 149, 1:50,000 series, (Solid Edition), Southampton, UK.

Jahoda, R., Andrews, J. R., & Foscer, R. P. (1989). Structural controls of Monterosso and other gold deposits in Northwest Spain in fractures, jogs and hot jogs. *Transactions of the Institution of Mining and Metallurgy. (Section B: Applied Earth Science)*, *98*, l–6.

Jia, Y. (2002). *Nitrogen isotope characteristics of orogenic lode gold deposits and terrestrial reservoirs*. Unpublished PhD thesis, University of Saskatchewan.

Kelly, P. G., Sanderson, D. J., & Peacock, D. C. P. (1998). Linkage and evolution of conjugate strike-slip fault zones in limestones of Somerset and Northumbria. *Journal of Structural Geology*, *20*(11), 1477–1493.

Keppie, J. D., Boyle, R. W., & Haynes, S. J. (1986). *Turbidite-hosted gold deposits* (p. 32). Geological Association of Canada. Special Paper.

Kisch, H. J. (1987). Correlation between indicators of very low grade metamorphism. In M. Frey (Ed.), *Low temperature metamorphism* (pp. 227–300). Blackie.

Kokelaar, B. P. (1979). Tremadoc to Llanvirn volcanism on the south side of the Harlech dome (Rhobell Fawr), North Wales. In A. L. Harris, C. H. Holland, & B. E. Leake (Eds.), *The Caledonides of the British Isles—Reviewed* (Vol. 8, pp. 591–596). Geological Society, London, Special Publications.

Kontak, D. J., Smith, P. K., Kerrich, R., & Williams, P. F. (1990). Integrated model for Meguma group lode gold deposits, Nova Scotia, Canada. *Geology*, *18*(3), 238–242.

Kříbek, B., Sýkorová, I., Machovič, V., Knésl, I., Laufek, F., & Zachariáš, J. (2015). The origin and hydrothermal mobilization of carbonaceous matter associated with Paleoproterozoic orogenic-type gold deposits of West Africa. *Precambrian Research*, *270*, 300–317.

Kydd, R., & Levinson, A. (1986). Ammonium halos in lithogeochemical exploration for gold at the horse canyon carbonate-hosted deposit, Nevada, U.S.A.: Use and limitations. *Applied Geochemistry*, *1*(3), 407–417.

Large, R. R., Bull, S. W., & Maslennikov, V. (2011). A carbonaceous sedimentary source rock model for Carlin-type and orogenic gold deposits. *Economic Geology*, *106*, 331–358.

Large, R. R., Halpin, J. A., Danyushevsky, L. V., Maslennikov, V., Bull, S. W., Long, J. A., Gregory, D. D., Lounejeva, E., Lyons, T. W., Sack, P. J., McGoldrick, P. J., & Calver, C. R. (2014). Trace element content of sedimentary pyrite as a new proxy for deep-time ocean–atmosphere evolution. *Earth and Planetary Science Letters*, *389*, 209–220.

Laughrey, C. D., Ruble, T. E., Lemmens, H., Kostelnik, J., Butcher, A. R., Walker, G., & Knowles, W. (2011). Black shale diagenesis: Insights from integrated high-definition analyses of post-mature Marcellus formation rocks, Northeastern Pennsylvania. AAPG Annual Convention and Exhibition, Houston, Texas, USA.

Lin, Z., Sun, X., Peckmann, J., Lu, Y., Xu, L., Strauss, H., Zhou, H., Gong, J., Lu, H., & Teichert, B. M. A. (2016). How sulfate-driven anaerobic oxidation of methane affects the sulfur isotopic composition of pyrite: A SIMS study from the South China Sea. *Chemical Geology*, *440*, 26–41.

Martínez Poyatos, D. M., Nieto, F., Azor, A., & Simancas, J. F. (2001). Relationships between very low-grade metamorphism and tectonic deformation: Examples from the southern central Iberian zone (Iberian massif, Variscan Belt). *Journal of the Geological Society*, *158*(6), 953–968.

Mason, J. S., Bevins, R. E., & Alderton, D. H. M. (2002). Ore mineralogy of the mesothermal gold lodes of the Dolgellau Gold Belt, North Harlech. *Transactions of the Institution of Mining and Metallurgy. (Section B: Applied Earth Science)*, *111*, 203–214.

Mason, J. S., Fitches, W. R., & Bevins, R. E. (1999). Evidence for a pre-tectonic origin for the auriferous vein-type mineralisation in the Dolgellau gold-belt, North Harlech. *Transactions of the Institution of Mining and Metallurgy (Section B, Applied Earth Science)*, *108*, 45–52.

Merriman, R., & Roberts, B. (2000). Low-grade metamorphism in the Scottish southern uplands terrane: Deciphering the patterns of accretionary burial, shearing and cryptic aureoles. *Earth and Environmental*

Science Transactions of the Royal Society of Edinburgh, *91*(3–4), 521–537.

Merriman, R. J. (2005). Clay minerals and sedimentary basin history. *European Journal of Mineralogy*, *17*, 7–20.

Merriman, R. J. (2006). Clay mineral assemblages in British lower Palaeozoic mudrocks. *Clay Minerals*, *41*, 473–512.

Merriman, R. J., Roberts, B., & Peacor, D. R. (1990). A transmission electron microscope study of white mica crystallite size distribution in a mudstone to slate transitional sequence, North Harlech. *Contributions to Mineralogy and Petrology*, *106*, 27–40.

Meyer, F. M., & Ridgway, J. (1991). Ammonium in Witwatersrand reefs: A possible indicator of metamorphic fluid flow. *South African Journal of Geology*, *94*(5/6), 343–347.

Morrison, T. A. (1975). Goldmining in Western Merioneth. *Llandysul*, *Harlech*, *the Merioneth Historical Society*.

Mortensen, J. K., Craw, D., MacKenzie, D. J., Allan, M. M., & Chapman, R. J. (2022). Concepts and revised models for Phanerozoic orogenic gold deposits. In T. Torvela, J. S. Lambert-Smith, & R. J. Chapman (Eds.), *Recent advances in understanding gold deposits: From orogeny to alluvium* (Vol. 516). Geological Society. https://doi.org/10.1144/SP516-2021-39

Naden, J., & Shepherd, T. J. (1989). Role of methane and carbon dioxide in gold deposition. *Nature*, *342*, 793–795.

Nicholson, R., & Pollard, D. D. (1985). Dilation and linkage of echelon cracks. *Journal of Structural Geology*, *7*(5), 583–590.

Nieto, F. (2002). Characterization of coexisting NH_4^- and K-micas in very low-grade metapelites. *American Mineralogist*, *87*, 205–216.

Noronha, F., Cathelineau, M., Boiron, C., Banks, D. A., Dória, A., Ribeiro, M. A., Nogueira, P., & Guedes, A. (2000). A three stage fluid flow model for Variscan gold metallogenesis in northern Portugal. *Journal of Geochemical Exploration*, *71*(2), 209–224.

Olson, J. E., & Pollard, D. D. (1991). The initiation and growth of en échelon veins. *Journal of Structural Geology*, *13*(5), 95–608.

Ottolini, L. P., Scordari, F., & Mesto, E. (2014). A new application of SIMS to the analysis of nitrogen in mica minerals: Tobelite. IOP Conference Series. *Materials Science and Engineering*, *55*, 012014.

Phillips, G., & Powell, R. (2010). Formation of gold deposits: A metamorphic devolatilization model. *Journal of Metamorphic Geology*, *28*, 689–718.

Phillips, G. N., & Evans, K. A. (2004). Role of CO_2 in the formation of gold deposits. *Nature*, *429*, 860–863.

Pitcairn, I. K., Leventis, N., Beaudoin, G., Faure, S., Guilmette, C., & Dubé, B. (2021). A metasedimentary source of gold in Archean orogenic gold deposits. *Geology*, *49*(7), 862–866. https://doi.org/10.1130/G48587.1

Pitcairn, I.K., Leventis, N. G., Beaudoin, G., & Dubé B. (2017). A metasedimentary source of gold in the Abitibi belt? Proceedings of the 14th Biennial SGA Meeting, Quebec, 20–23 august, Volume 1, 91–94.

Pitcairn, I. K., Skelton, A., & Wolgemuth-Uebewasser, C. C. (2015). Mobility of gold during metamorphism of the Dalradian in Scotland. *Lithos*, *233*, 69–88.

Pitcairn, I. K., Teagle, D. A. H., Craw, D., Olivo, G. R., Kerrich, R., & Brewer, T. S. (2006). Sources of metals and fluids in orogenic gold deposits: Insights from the Otago and alpine schists, New Zealand. *Economic Geology*, *101*, 1525–1546.

Pitcairn, I. K., Teagle, D. A. H., Kerrich, R., Craw, D., & Brewer, T. S. (2005). The behaviour of nitrogen and nitrogen isotopes during metamorphism and mineralization: Evidence from the Otago and alpine schists, New Zealand. *Earth and Planetary Science Letters*, *233*, 229–246.

Pizarras, C. (1998). *Product technical specification*. Cupa Pizarras.

Platten, I. M., & Dominy, S. C. (1999). Re-evaluation of quartz vein history in the Dolgellau Gold-Belt, North Wales, United Kingdom. *Geological Journal*, *34*, 369–391.

Platten, I.M., & Dominy, S.C. (2009). Geological mapping in the evaluation of structurally controlled gold veins: A case study from the Dolgellau gold belt, North Harlech, UK. Proceedings World Gold Conference, Southern African Institute of Mining and Metallurgy, *S60*, 151–168.

Pokrovski, G. S., Akinfiev, N. N., Borisova, A. Y., Zotov, A. V., & Kouzmanov, K. (2014). Gold speciation and transport in geological fluids: Insights from experiments and physical-chemical modelling. In P. S. Garofalo & J. R. Ridley (Eds.), *Gold-Transporting Hydrothermal Fluids in the Earth's Crust* (Vol. 402, pp. 9–70). Geological Society, London, Special Publications.

Radke, A. S. (1985). *Geology of the Carlin gold deposit* (p. 1267). Nevada.

Rice, R., & Sharp, G. (1976). Copper mineralisation in the forest of coed-y-Brenin, Harlech. *Transactions of the Institution of Mining and Metallurgy (Section B, Applied Earth Science)*, *85*, 1–13.

Ridgway, J., Appleton, J. D., & Levinson, A. A. (1990). Ammonium geochemistry in mineral exploration—A comparison of results from the American cordilleras and the Southwest Pacific. *Applied Geochemistry*, *5*(4), 475–489.

Roberts, B., Evans, J. A., Merriman, R. J., Smith, M., Bevins, R. E., & Robinson, D. (1989). Discussion on: Bevins, R.E., & Robinson, D., (1988), Low grade metamorphism of the Welsh basin Lower Proterozoic succession: an example of diastathermal metamorphism? *Journal of the Geological Society of London*, *146*(5), 885–890.

Roberts, B., Merriman, R., Hirons, S. R., Fletcher, C., & Wilson, D. (1996). Synchronous very low-grade metamorphism, contraction and inversion in the central part of the welsh lower Palaeozoic Basin. *Journal of the Geological Society*, *153*, 277–285.

Roberts, B., & Merriman, R. J. (1985). The distinction between Caledonian burial and regional metamorphism in metapelites from North Wales. *Journal of the Geological Society of London*, *142*(5), 615–624.

Roberts, B., Merriman, R. J., & Pratt, W. (1991). The relative influences of strain, lithology and stratigraphical depth on white mica (illite) crystallinity in mudrocks from the district centred on the Corris Slate Belt, Gwynedd-Powys. *Geological Magazine*, *128*, 633–645.

Rodríguez Sastre, M. A., & González Menéndez, L. (2011). Stratigraphy and structure of the uppermost part of the Luarca Formation in Alto Bierzo, Leon (Ordovician, NW Spain). In J. C. Gutiérrez-Marco, I. Isabel Rábano, & D. García-Bellido (Eds.), Cuadernos del Museo Geominero, 14 *Ordovician of the World* (pp. 473–481). Instituto Geológico y Minero de España.

Rothery, E. (1988). En échelon vein array development in extension and shear. *Journal of Structural Geology*, *10*(1), 63–71.

Rubio-Pascual, F. J., Arenas, R., Martínez Catalán, J. R., Rodríguez Fernández, L. R., & Wijbrans, J. R. (2013). Thickening and exhumation of the Variscan roots in the Iberian central system;Tectonothermal processes and $^{40}Ar/^{39}Ar$ ages. *Tectonophysics*, *587*, 207–221.

Ryan, R. J., & Smith, P. K. (1998). A review of the mesothermal gold deposits of the Meguma group, Nova Scotia, Canada. *Ore Geology Reviews*, *13*(1–5), 53–183.

Sack, P. J., Large, R. R., & Gregory, D. D. (2018). Geochemistry of shale and sedimentary pyrite as a proxy for gold fertility in the Selwyn basin area, Yukon. *Mineralium Deposita*, *53*, 997–1018.

Schmidt, C., & Watenphul, A. (2010). Ammonium in aqueous fluids to 600°C, 1.3 GPa: A spectroscopic study on the effects on fluid properties, silica solubility, and K-feldspar to muscovite reactions. *Geochimica et Cosmochimica Acta*, *74*(23), 6852–6866.

Scott, R. J., Meffre, S., Woodhead, J., Gilbert S. E, Gilbert, S. E., Berry, R. E., & Emsbo, P. (2009). Development of framboidal pyrite during diagenesis, low-grade regional metamorphism, and hydrothermal alteration. *Economic Geology*, *104*, 1145–1168.

Shepherd, T. J., Bottrell, S., & Miller, M. F. (1991). Fluid inclusion volatiles as an exploration guide to black shale-hosted gold deposits, Dolgellau gold belt, North Harlech, UK. *Journal of Geochemical Exploration*, *42*, 5–24.

Shepherd, T. J., & Bottrell, S. H. (1993). Dolgellau Gold-belt, Harlech district, North Harlech. In R. A. D. Pattrick & D. A. Polya (Eds.), *Mineralisation in the British Isles* (pp. 187–205). Chapman and Hall.

Sibson, R. H., Robert, F., & Poulsen, K. H. (1988). High-angle reverse faults, fluid-pressure cycling, and mesothermal gold-quartz deposits. *Geology*, *16*, 551–555.

Smith, I. F., & McCann, D. M. (1978). Geophysical investigations. In P. M. Allen & A. A. Jackson (Eds.), *Bryn-Teg borehole, North Wales* (Vol. 61, p. 51). Bulletin, Geological Survey.

Smith, J. R. (1977). *Mines of Merioneth*. Northern Mine Research Society.

Smolarek, J., Trela, W., Bond, D., & Marynowski, L. (2017). Lower Wenlock black shales in the northern holy Cross Mountains, Poland: Sedimentary and geochemical controls on the Ireviken event in a deep marine setting. *Geological Magazine*, *154*(2), 247–264.

Spence-Jones, C. P., Jenkin, G. R. T., Boyce, A. J., Hill, N., & Sangster, C. J. S. (2018). Tellurium, magmatic fluids and orogenic gold: An early magmatic fluid pulse at Cononish gold deposit, Scotland. *Ore Geology Reviews*, *102*, 894–905.

Steadman, J. A., Large, R. R., Meffre, S., Olin, P. H., Danyushevsky, L. V., Gregory, D. D., Belousov, I., Lounejeva, E., Ireland, T. R., & Holden, P. (2015). Synsedimentary to early diagenetic gold in black shale-hosted pyrite nodules at the Golden mile deposit, Kalgoorlie, Western Australia. *Economic Geology*, *100*, 1157–1191.

Stüeken, E. E., Boocock, T. J., Robinson, A., Mikhail, S., & Johnson, B. W. (2021). Hydrothermal recycling of sedimentary ammonium into oceanic crust and the Archean Ocean at 3.24 Ga. *Geology*, *49*(7), 822–826. https://doi.org/10.1130/G48844.1

Suárez, A., Barba, P., Heredia, N., & Rodríguez Fernández, L.R. (1994). Mapa Geológico de la Provincia de León. Escala 1:200.000. *Instituto Tecnológico Geominero de España* (ITGE).

Tomkins, A. G. (2010). Windows of metamorphic sulfur liberation in the crust: Implications for gold deposit genesis. *Geochimica et Cosmochimica Acta*, *74*, 3246–3259.

Tomkins, A. G. (2013). On the source of orogenic gold. *Geology*, *41*(12), 255–1256.

Villa, L., Corretgé, L. G., Arias, D., & Suárez, O. (2004). Los depósitos volcanoclásticos sineruptivos del paleozoico inferior del área de lago-Fontarón (Lugo, España). *Trabajos de Geologia*, *24*, 185–205.

Voldman, G. G., & Toyos, J. M. (2019). Taxonomy, biostratigraphy and biofacies of an upper Ordovician (Katian) conodont fauna from the Casaio formation, Northwest Spain. *Bulletin of Geosciences*, *94*(4), 455–478.

Wacey, D., Kilburn, M., Saunders, M., Cliff, J., Kong, C., Liu, A. G., Matthews, J. J., & Brasier, M. (2014). Uncovering framboidal pyrite biogenicity using nano-scale CN_{org} mapping. *Geology*, *43*(1), 27–30.

Wang, H., Ma, Y., & Zhou, J. (2012). Diagenesis and very low grade metamorphism in a 7,012 m-deep well, Hongcan 1, eastern Tibetan plateau. *Swiss Journal of Geosciences*, *105*, 249–261.

Williams, L. B., Ferrell, R. E., Hutcheon, I., Bakel, A. J., Walsh, M. M., & Krouse, H. R. (1995). Nitrogen isotope geochemistry of organic matter and minerals during diagenesis and hydrocarbon migration. *Geochimica et Cosmochimica Acta*, *59*(4), 765–779.

Wilson, P. N., Parry, W. T., & Nash, W. P. (1992). Characterization of hydrothermal tobelitic veins from black shale, Oquirrh Mountains, Utah. *Clays and Clay Minerals*, *40*, 405–420.

Wood, S. A. (1996). The role of humic substances in the transport and fixation of metals of economic interest (Au, Pt, Pd, U, V). *Ore Geology Reviews*, *11*, 1–31.

Wu, Y.-F., Evans, K. A., Fisher, L. A., Zhou, M.-F., Hud, S.-Y., Fougerouse, D., Large, R. R., & Li, J.-W. (2020). Distribution of trace elements between carbonaceous matter and sulfides in a sediment-hosted orogenic gold system. *Geochimica et Cosmochimica Acta*, *276*, 345–362.

Wu, Y.-F., Evans, K. A., Li, J.-W., Fougerouse, D., Large, R. R., & Guagliardo, P. (2019). Metal remobilization and ore-fluid perturbation during episodic replacement of auriferous pyrite from an epizonal orogenic gold deposit. *Geochimica et Cosmochimica Acta*, *245*, 98–117.

Zhong, R., Brugger, J., Tomkins, A. G., Chen, Y., & Li, W. (2015). Fate of gold and base metals during metamorphic devolatilization of a pelite. *Geochimica et Cosmochimica Acta*, *171*, 338–352.

SUPPORTING INFORMATION

Additional supporting information can be found online in the Supporting Information section at the end of this article.

How to cite this article: Cunningham, J. K., Gómez-Fernández, F., González-Menéndez, L., & Beard, A. D. (2022). Black shales and mesozonal quartz vein-hosted Au: The Truchas Syncline, Spain and the Harlech Dome, Wales, a comparative study. *Geological Journal*, 1–23. https://doi.org/10.1002/gj.4581